

Supporting Information

Ti₃C₂T_x MXene Nanosheets Hybridized with Bacteriochlorin-Carotenoid Conjugates for Photocatalytic Hydrogen Evolution

Xiaoli Sun,[†] Yuanlin Li,[†] Xiao-Feng Wang,^{*,†} Ritsuko Fujii,^{‡,§} Yumiko Yamano,[¶] Osamu Kitao,[⊥]
and Shin-ichi Sasaki,^{*,∇}

[†]Key Laboratory of Physics and Technology for Advanced Batteries (Ministry of Education),
College of Physics, Jilin University, Changchun 130012, P. R. China

[‡]Graduate School of Science, and [§]Research Center for Artificial Photosynthesis, Osaka City
University, Sumiyoshi, Osaka 558-8585, Japan

[¶]Laboratory of Organic Chemistry for Life Science, Kobe Pharmaceutical University, Kobe,
Hyogo 658-8558, Japan

[⊥] Global Zero Emission Research Center (GZR), National Institute of Advanced Industrial
Science and Technology (AIST), Tsukuba West, 16-1 Onogawa, Tsukuba, Ibaraki 305-8569,
Japan

[∇]Department of Medical Bioscience, Nagahama Institute of Bio-Science and Technology,
Nagahama, Shiga 526-0829, Japan

E-mail: xf_wang@jlu.edu.cn ; s_sasaki@nagahama-i-bio.ac.jp

List of contents

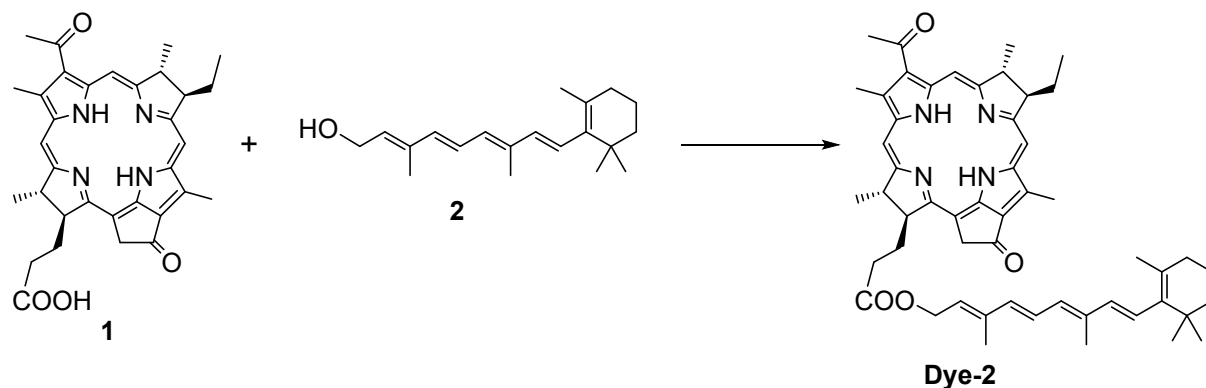
Synthetic details and characterization data of Dyes-2-6 .		S3–S12
Figures S1–S6	Energy-optimized structures of Dyes-1-6 .	S13–S18
Figures S7–S16	¹ H- and ¹³ C-NMR spectra of Dyes-2-6 .	S19–S23
Figures S17–S21	HRMS spectra of Dyes-2-6 .	S24–S26
Figure S22	UV-VIS absorption spectra of carotenols 3-5 .	S27
Figure S23	Cyclic voltammograms of Dyes-1-6 .	S28
Figure S24-S26	Theoretical absorption spectra and oscillator strength of Dyes-1-6 .	S29-S31
Figure S27	Energy gaps concerning main contributed frontier orbitals describing the electron excitations in the carotenoid moieties of Dyes-3-6 .	S32
Figure S28	The optimized structure, HOMO+1, and LUMO+1 of Dye-4	S33
Figure S29	The H ₂ production optimization of each composite.	S34
Figure S30	EDX mapping of Ti-C-N in Dye-1@Ti₃C₂T_x .	S35
Figure S31	EDX mapping of Ti-C-Al in Ti ₃ AlC ₂ and Ti ₃ C ₂ T _x .	S36
Figure S32	FT-IR spectra of Ti ₃ C ₂ T _x , Dye-4 , and Dye-4@Ti₃C₂T_x .	S37
Table S1	The fitting data of Nyquist plots.	S38

General

Electronic absorption spectra were recorded on Shimadzu UV-2550 spectrometer. All melting points were measured with a Yanagimoto micro melting apparatus and were uncorrected. HRMS were measured by a 7 Tesla Solarix FT-ICR-MS (Bruker Daltonik, Bremen, Germany) in positive ion mode with DCTB (*trans*-2-[3-(4-*tert*-butylphenyl)-2-methyl-2-propenylidene] malononitrile) dissolved in tetrahydrofuran. ¹H- and ¹³C-NMR spectra were recorded on a JEOL ECX-500 spectrometer in CDCl₃, and chemical shifts are reported relative to the residual solvent peaks [δ = 7.26 ppm (CHCl₃) for ¹H-NMR (500 MHz) and 77.0 ppm (¹³CDCl₃) for ¹³C-NMR (125 MHz)]. Proton peaks were assigned by ¹H-¹H COSY as well as ROESY spectra, and carbon peaks except for quaternary peaks were assigned by DEPT and HMQC spectra. Flash column chromatography (FCC) was performed with silica gel (Merck, Kieselgel 60) or aluminium oxide (Merck, Aluminium oxide 90, active neutral (activity stage I) 0.063-0.200 mm) deactivated with 5% H₂O. PLC was done with silica gel plate (Merck, Kieselgel 60, 1 mm).

Bacteriopyropheorbide-*a* (**1**)^{S1}, methyl bacteriopyropheorbide-*a* (**Dye-1**)^{S1}, and β -apo-8'-carotenol (**3**)^{S2} were synthesized according to literature procedures. Retinol **2** was purchased from Nacalai Tesque Co., Japan. Carotenoid analogs **4** and **5** were prepared according to the methods for the total synthesis of siphonaxanthin and lodoxanthin, respectively, and the synthetic details will be reported in a separate paper. Other solvents and reagents were used as purchased without further purification. All synthetic procedures were done in the dark.

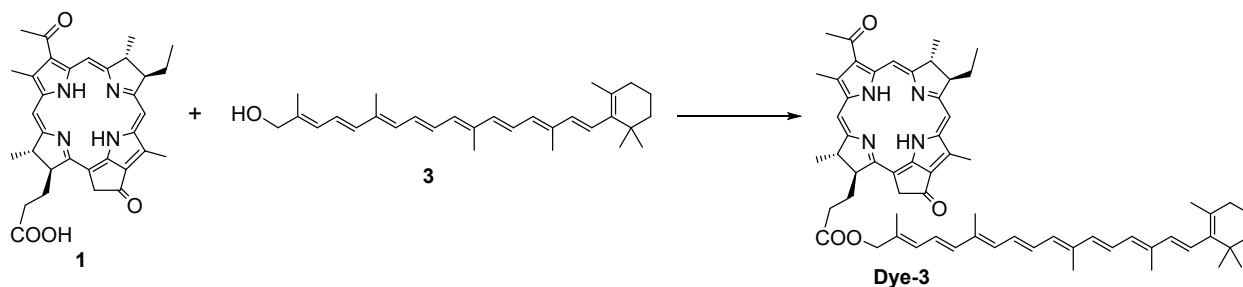
Bacteriopyropheophorbide-*a* retinol ester (**Dye-2**)



To a solution of bacteriopyropheophorbide-*a* (100 mg, 0.18 mmol) and retinol **2** (100 mg, 0.35 mmol) in CH₂Cl₂ (30 mL) was added 4-dimethylaminopyridine (DMAP, 105 mg, 0.86 mmol) and 1-(3-dimethylaminopropyl)-3-ethylcarbodiimide hydrochloride (EDC·HCl, 121 mg, 0.63 mmol), and the mixture was stirred for 12 h at room temperature. The mixture was poured into aqueous diluted HCl, extracted with CH₂Cl₂, washed with brine, and concentrated in vacuo. The crude product was purified by FCC (Al₂O₃, CH₂Cl₂) to give **Dye-2** (148 mg, quant.) as a dark brown solid: VIS (THF) λ_{\max} 751 (rel. 0.56), 679 (0.08), 529 (0.22), 385 (0.49), 358 nm (1.00); ¹H-NMR Bacteriochlorin moiety: δ = 9.02 (1H, s, 5-H), 8.47 (1H, s, 10-H), 8.44 (1H, s, 20-H), 5.12, 4.94 (each 1H, d, J = 20 Hz, 13¹-CH₂), 4.70-4.60 (2H, m, 17²-COOCH₂), 4.34-4.28 (2H, m, 7-, 18-H), 4.15 (1H, br-d, J = 8 Hz, 17-H), 4.05-4.02 (1H, m, 8-H), 3.50 (3H, s, 2-CH₃), 3.45 (3H, s, 12-CH₃), 3.17 (3H, s, 3¹-CH₃), 2.65-2.50, 2.31-2.24 (each 2H, m, 17-CH₂CH₂) 2.39-2.34, 2.11-2.05 (each 1H, m, 8-CH₂), 1.81 (3H, d, J = 7 Hz, 7-CH₃), 1.74 (3H, d, J = 8 Hz, 18-CH₃), 1.12 (3H, t, J = 8 Hz, 8¹-CH₃), 0.35, -1.03 (each 1H, s, NH \times 2), Carotenoid moiety: δ = 6.60 (1H, dd, J = 11 Hz, 11''-H), 6.18 (each 1H, d, J = 15 Hz, 7''-, 12''-H), 6.10 (1H, d, J = 16 Hz, 8''-H), 6.06 (1H, d, J = 12 Hz, 10''-H), 5.45 (1H, t, J = 7 Hz, 14''-H), 2.01 (2H, t, J = 6 Hz, 4''-H₂), 1.94 (each 3H, s, 19''-, 20''-H₃), 1.71 (3H, s, 18''-H₃), 1.61 (2H, m, 3''-H₂), 1.46 (2H, m, 2''-H₂),

1.02 (each 3H, s, 16"-, 17"-H₃); ¹³C-NMR quaternary carbon: δ = 199.1, 195.6, 172.9, 170.4, 168.5, 163.6, 157.3, 147.2, 139.2, 139.1, 137.8, 137.50, 136.6, 136.5, 135.7, 132.7, 130.2, 129.3, 120.9, 109.1, 34.2, Bacteriochlorin moiety: δ = 99.1 (C10), 97.2 (C5), 95.9 (C20), 61.3 (C17⁵), 55.0 (C8), 51.2 (C17), 49.5, 48.7 (C7, 18), 47.7 (C13²), 33.3 (C3²), 31.0, 30.1, 29.9 (C8¹, 17¹, 17²), 23.0 (C7¹, 18¹), 13.4 (C2¹), 11.5 (C12¹), 10.7 (C8²), Carotenoid moiety: δ = 137.5 (C8"), 135.6 (C12"), 129.9 (C10"), 127.0 (C7"), 125.8 (C11"), 124.1 (C14"), 39.6 (C2"), 33.0 (C4"), 19.2 (C3"), 28.9 (C16", 17"), 21.7 (C18"), 12.69 (C19"), 12.67 (C20"); HRMS *m/z* 820.4921 (M⁺), calcd for C₅₃H₆₄N₄O₄⁺: 820.4922.

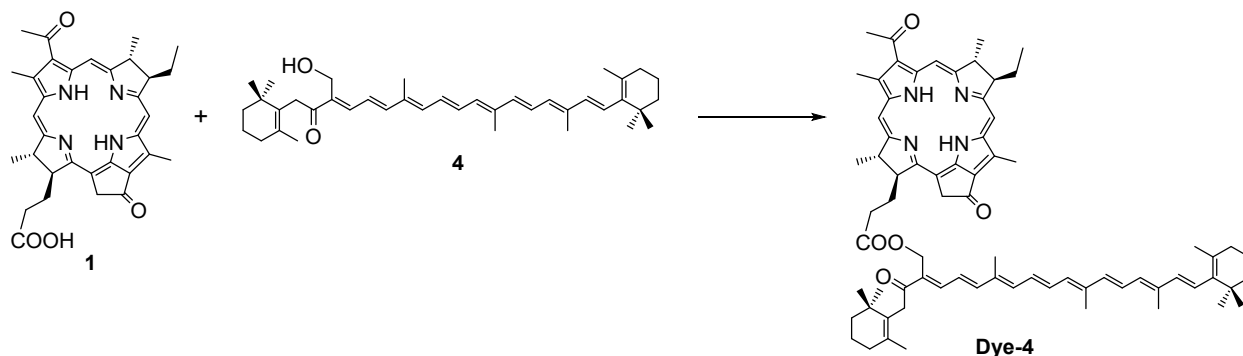
Bacteriopyropheophorbide-*a* β -apo-8'-carotenol ester (**Dye-3**)



Condensation reaction of bacteriopyropheophorbide-*a* **1** (58 mg, 0.10 mmol) and β -apo-8'-carotenol **3** (60 mg, 0.14 mmol) in CH₂Cl₂ (30 mL) in the presence of DMAP (60 mg, 0.49 mmol) and EDC·HCl (68 mg, 0.35 mmol) gave **Dye-3** after FCC (Al₂O₃, hexane-CH₂Cl₂ = 1:1 to 0:1) as a brown solid (60 mg, 60%): VIS (THF) λ_{max} 751 (rel. 0.56), 680 (0.08), 529 (0.23), 458 (0.63), 432 (0.72), 386 (0.74), 359 nm (1.00); ¹H-NMR Bacteriochlorin moiety: δ = 9.01 (1H, s, 5-H), 8.48 (1H, s, 10-H), 8.43 (1H, s, 20-H), 5.11, 4.94 (each 1H, d, *J* = 20 Hz, 13¹-CH₂), 4.49, 4.40 (each 1H, d, *J* = 13 Hz, 17²-COOCH₂), 4.34-4.28 (2H, m, 7-, 18-H), 4.16 (1H, br-d, *J* = 8

Hz, 17-H), 4.05-4.02 (1H, m, 8-H), 3.50 (3H, s, 2-CH₃), 3.45 (3H, s, 12-CH₃), 3.16 (3H, s, 3¹-CH₃), 2.66-2.53, 2.39-2.27, 2.11-2.05 (2H+3H+1H, m, 8-CH₂, 17-CH₂CH₂), 1.81 (3H, d, *J* = 7 Hz, 7-CH₃), 1.74 (3H, d, *J* = 7 Hz, 18-CH₃), 1.12 (3H, t, *J* = 7 Hz, 8¹-CH₃), 0.34, -1.04 (each 1H, s, NH × 2), Carotenoid moiety: δ = 6.65 (1H, dd, *J* = 12, 15 Hz, 11''-H), 6.60 (1H, m, 15'-H), 6.58 (1H, m, 15''-H), 6.35 (1H, dd, *J* = 12, 15 Hz, 11'-H), 6.34 (1H, d, *J* = 15 Hz, 12''-H), 6.24 (1H, d, *J* = 15 Hz, 12'-H), 6.22 (1H, d, *J* = 11 Hz, 14'-H), 6.19 (1H, d, *J* = 12 Hz, 14''-H), 6.18 (1H, d, *J* = 16 Hz, 7''-H), 6.15 (1H, d, *J* = 12 Hz, 10''-H), 6.13 (1H, d, *J* = 16 Hz, 8''-H), 6.04 (1H, d, *J* = 11 Hz, 10'-H), 2.02 (2H, t, *J* = 7 Hz, 4''-H), 1.98 (3H, s, 19''-H₃), 1.96 (3H, s, 20''-H₃), 1.89 (3H, s, 20'-H₃), 1.72 (3H, s, 18''-H₃), 1.68 (3H, s, 19'-H₃), 1.64-1.59 (2H, m, 3''-H₂), 1.48-1.46 (2H, m, 2''-H₂), 1.03 (each 3H, s, 16'', 17''-H₃); ¹³C-NMR quaternary carbon: δ = 199.1, 195.6, 172.9, 170.4, 168.5, 163.6, 157.2, 147.2, 139.1, 137.9, 137.5, 136.7, 136.5, 136.1, 135.75, 135.70, 132.7, 131.5, 130.2, 129.4, 121.0, 109.1, 34.3, Bacteriochlorin moiety: δ = 99.2 (C10), 97.2 (C5), 95.9 (C20), 70.0 (C17^s), 55.0 (C8), 51.2 (C17), 49.5, 48.7 (C7, 18), 47.7 (C13²), 33.3 (C3²), 31.0, 30.2, 29.9 (C8¹, 17¹, 17²), 23.0 (C7¹, 18¹), 13.4 (C2¹), 11.5 (C12¹), 10.7 (C8²), Carotenoid moiety: δ = 138.5 (C12'), 137.7 (C8''), 137.1 (C12''), 133.0 (C14''), 132.2 (C14'), 130.8 (C10''), 130.4(C15'), 129.6 (C15''), 129.2 (C10'), 126.7 (C7''), 125.2 (C11''), 123.2 (C11'), 39.6 (C2''), 33.1 (C4''), 19.3 (C3''), 29.0 (C16'', 17''), 21.8 (C18''), 14.7 (C19''), 12.8, 12.75, 12.71 (C20', 19'', 20''); HRMS *m/z* 952.5861 (M⁺), calcd for C₆₃H₇₆N₄O₄⁺: 952.5861.

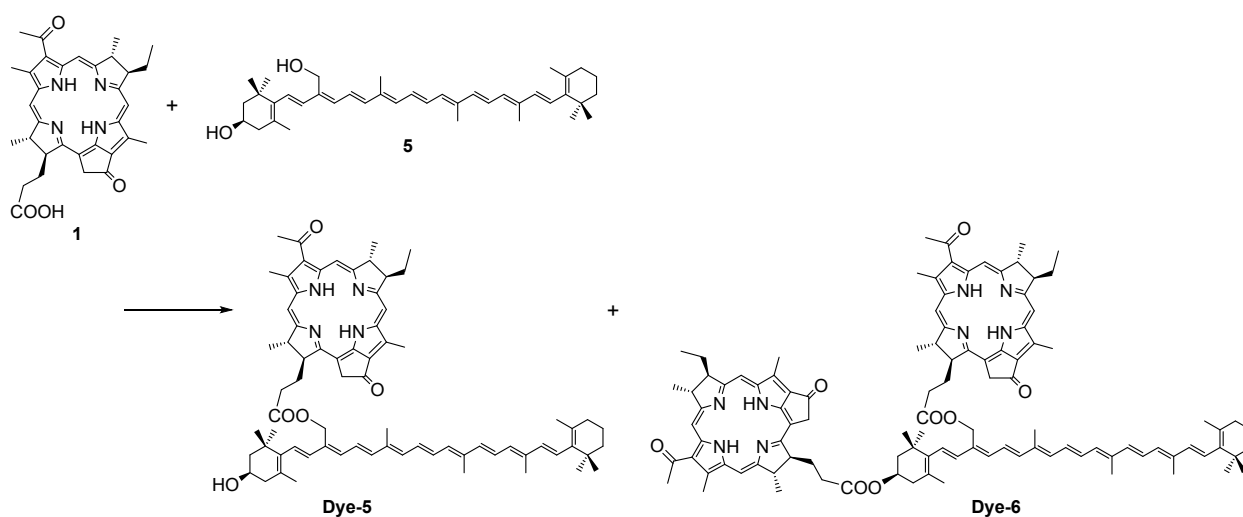
Bacteriochlorin-carotenoid dyad (**Dye-4**)



Condensation reaction of bacteriopyropheophorbide-*a* **1** (55 mg, 0.10 mmol) and carotenol **4** (siphonaxanthin analog, 57 mg, 0.10 mmol) in CH₂Cl₂ (30 mL) in the presence of DMAP (49 mg, 0.40 mmol) and EDC·HCl (58 mg, 0.30 mmol) gave **Dye-4** after PLC (SiO₂, acetone-CH₂Cl₂ = 1:19) as a dark brown solid (50 mg, 45%): VIS (THF) λ_{\max} 751 (rel. 0.58), 680 (0.09), 466 (0.85), 389 (0.67), 359 nm (1.00); ¹H-NMR Bacteriochlorin moiety: δ = 9.00 (1H, s, 5-H), 8.46 (1H, s, 10-H), 8.41 (1H, s, 20-H), 5.05, 4.90 (each 1H, d, J = 20 Hz, 13¹-CH₂), 5.05-4.99 (2H, m, 17²-COOCH₂), 4.32-4.25 (2H, m, 7-, 18-H), 4.10 (1H, br-d, J = 9 Hz, 17-H), 4.04-4.01 (1H, m, 8-H), 3.50 (3H, s, 2-CH₃), 3.43 (3H, s, 12-CH₃), 3.16 (3H, s, 3¹-CH₃), 2.64-2.48, 2.26-2.16 (each 2H, m, 17-CH₂CH₂), 2.39-2.34, 2.11-2.06 (each 1H, m, 8-CH₂), 1.80 (3H, d, J = 7 Hz, 7-CH₃), 1.70 (3H, d, J = 7 Hz, 18-CH₃), 1.12 (3H, t, J = 7 Hz, 8¹-CH₃), 0.31, -1.07 (each 1H, s, NH \times 2), Carotenoid moiety: δ = 7.36 (1H, d, J = 11 Hz, 10'-H), 6.71 (1H, dd, J = 11, 15 Hz, 15'-H), 6.71 (1H, d, J = 15 Hz, 12'-H), 6.70 (1H, dd, J = 11, 15 Hz, 15''-H), 6.62 (1H, dd, J = 12, 15 Hz, 11'-H), 6.45 (1H, dd, J = 12, 14 Hz, 11''-H), 6.36 (1H, d, J = 12 Hz, 10''-H), 6.35 (1H, d, J = 15 Hz, 12''-H), 6.22 (1H, d, J = 16 Hz, 8''-H), 6.20 (1H, d, J = 12 Hz, 14''-H), 6.17 (1H, d, J = 12 Hz, 14'-H), 6.15 (1H, d, J = 16 Hz, 7''-H), 3.40 (2H, br-s, 7'-H₂), 2.03 (2H, t, J = 6 Hz, 4''-H₂), 1.99 (3H, s, 19''-H₃), 1.98 (3H, s, 20''-H₃), 1.90 (2H, t, J = 6 Hz, 4'-H₂), 1.80 (3H, s, 20'-H₃), 1.73 (3H,

s, 18''-H₃), 1.65-1.60 (2H, m, 3''-H₂), 1.56-1.51 (2H, m, 3'-H₂), 1.49-1.46 (2H, m, 2''-H₂), 1.35-1.33 (2H, m, 2'-H₂), 1.33 (3H, s, 18'-H₃), 1.04 (each 3H, s, 16'', 17''-H₃), 0.78, 0.76 (each 3H, s, 16', 17'-H₃); ¹³C-NMR quaternary carbon: δ = 199.2, 197.2, 195.6, 172.9, 170.4, 168.5, 163.6, 157.3, 147.2, 139.1, 138.6, 137.9, 137.5, 136.9, 136.5, 135.7, 135.1, 132.6, 132.1, 130.8, 130.7, 130.2, 129.6, 120.9, 109.0, 34.4, 34.3, Bacteriochlorin moiety: 99.1 (C10), 97.2 (C5), 96.0 (C20), 57.9 (C17⁵), 55.0 (C8), 51.2 (C17), 49.4 (C7), 48.7 (C18), 47.7 (C13²), 33.4 (C3²), 31.0, 30.2, 30.0 (C8¹, 17¹, 17²), 13.4 (C2¹), 23.02, 22.97 (C7¹, 18¹), 11.7 (C12¹), 10.8 (C8²), Carotenoid moiety: δ = 147.4 (C12'), 142.7 (C10'), 137.8 (C14''), 137.6 (C7''), 136.8 (C12''), 133.1 (C15''), 131.9 (C8''), 130.6 (C10''), 129.1 (C15'), 127.2 (C14''), 126.2 (C11''), 122.2 (C11'), 39.6 (C2''), 39.1 (C2'), 37.0 (C7'), 33.1 (C4''), 32.4 (C4'), 19.3, 19.2 (C3'', 3'), 29.0 (C16'', 17''), 28.0 (C16', 17'), 21.8 (C18''), 20.4 (C18'), 12.9, 12.8, 12.7 (C20'', 20', 19''); HRMS *m/z* 1102.6898 (M⁺), calcd for C₇₃H₉₀N₄O₅⁺: 1102.6906.

Bacteriochlorin-carotenoid dyad (**Dye-5**) and triad (**Dye-6**)



Condensation reaction of bacteriopyropheophorbide-*a* **1** (80 mg, 0.14 mmol) and carotenol **5** (loroxanthin analog, 70 mg, 0.12 mmol) in CH₂Cl₂ (30 mL) in the presence of DMAP (85 mg, 0.70 mmol) and EDC·HCl (110 mg, 0.57 mmol) gave **Dye-5** (87 mg, 64%) and **Dye-6** (21 mg, 18%) after FCC (Al₂O₃, CH₂Cl₂) followed by PLC (SiO₂, acetone-CH₂Cl₂ = 1:9): **Dye-5**; VIS (THF) λ_{\max} 751 (rel. 0.57), 680 (0.08), 528 (0.27), 487 (0.60), 460 (0.70), 385 (0.65), 359 nm (1.00); ¹H-NMR Bacteriochlorin moiety: δ = 9.00 (1H, s, 5-H), 8.47 (1H, s, 10-H), 8.41 (1H, s, 20-H), 5.06, 4.91 (each 1H, d, J = 20 Hz, 13¹-CH₂), 4.99 (2H, s, 17²-COOCH₂), 4.33-4.26 (2H, m, 7-, 18-H), 4.12 (1H, br-d, J = 9 Hz, 17-H), 4.05-4.02 (1H, m, 8-H), 3.49 (3H, s, 2-CH₃), 3.44 (3H, s, 12-CH₃), 3.17 (3H, s, 3¹-CH₃), 2.63-2.53, 2.30-2.18 (each 2H, m, 17-CH₂CH₂), 2.40-2.35, 2.12-2.06 (each 1H, m, 8-CH₂), 1.80 (3H, d, J = 8 Hz, 7-CH₃), 1.71 (3H, d, J = 7 Hz, 18-CH₃), 1.12 (3H, t, J = 8 Hz, 8¹-CH₃), 0.31, -1.07 (each 1H, s, NH \times 2), Carotenoid moiety: δ = 6.66 (1H, dd, J = 12, 15 Hz, 11'-H), 6.63 (1H, dd, J = 12, 16 Hz, 15'-H), 6.62 (1H, dd, J = 12, 15 Hz, 11''-H), 6.51, (1H, dd, J = 12, 13 Hz, 15''-H), 6.39 (1H, d, J = 15 Hz, 12''-H), 6.34, (1H, d, J = 15 Hz, 12'-H), 6.27 (1H, d, J = 12 Hz, 14'-H), 6.24 (1H, d, J = 12 Hz, 10''-H), 6.21 (1H, d, J = 12 Hz, 14''-H), 6.19 (1H, d, J = 16 Hz, 7''-H), 6.15 (1H, d, J = 11 Hz, 10'-H), 6.14 (1H, d, J = 16 Hz, 8''-H), 6.09 (1H, d, J = 16 Hz, 7'-H), 5.96 (1H, d, J = 17 Hz, 8'-H), 3.86-3.80 (1H, m, 3'-H), 2.22-2.18 (1H, m, 4'-H _{α}), 2.02 (2H, t, J = 7 Hz, 4''-H₂), 1.98 (3H, s, 19''-H₃), 1.96 (3H, s, 20'-H₃), 1.89 (1H, d, J = 10 Hz, 4'-H _{β}), 1.85 (3H, s, 20''-H₃), 1.63-1.61 (2H, m, 3''-H₂), 1.61-1.58 (1H, m, 2'-H _{α}), 1.55 (3H, s, 18'-H₃), 1.48-1.46 (2H, m, 2''-H₂), 1.29 (1H, t, J = 12 Hz, 2'-H _{β}), 0.85 (3H, s, 17'-H₃), 0.83 (3H, s, 16'-H₃); ¹³C-NMR quaternary carbon: δ = 199.2, 195.6, 173.0, 170.4, 168.4, 163.6, 157.3, 147.2, 139.1, 137.9, 137.5, 137.4, 137.1, 136.4, 136.3, 135.9, 135.6, 132.7, 132.2, 130.2, 129.5, 126.6, 121.0, 109.1, 36.9, 34.3, Bacteriochlorin moiety: δ = 99.2 (C10), 97.2 (C5), 95.9 (C20), 58.6 (C17⁵), 55.1 (C8), 51.2 (C17), 49.4, 48.7 (C7, 18), 47.7 (C13²), 33.4 (C3²),

31.1, 30.2, 30.1 (C8¹, 17¹, 17²), 23.03, 22.97 (C7¹, 18¹), 13.4 (C2¹), 11.5 (C12¹), 10.8 (C8²), Carotenoid moiety: δ = 140.5 (C12^{''}), 137.7 (C8^{''}), 137.1 (C12[']), 135.2 (C8[']), 135.0 (C14[']), 134.1 (C10^{''}), 132.2 (C14^{''}), 131.0 (C11^{''}), 130.8 (C10[']), 129.6 (C15^{''}), 126.8 (C7^{''}), 126.6 (C7[']), 125.4 (C11[']), 123.3 (C15[']), 64.9 (C3[']), 48.1 (C2[']), 42.3 (C4[']), 39.6 (C2^{''}), 33.1 (C4^{''}), 19.3 (C3^{''}), 30.0 (C16[']), 29.0 (C16^{''}, 17^{''}), 28.5 (C17[']), 21.8 (C18^{''}), 21.4 (C18[']), 12.82, 12.77 (C19^{''}, 20^{''}, 20['], one peak is overlapping); HRMS m/z 1102.6906 (M⁺), calcd for C₇₃H₉₀N₄O₅⁺: 1102.6906. **Dye-6**; VIS (THF) λ_{\max} 751 (rel. 0.60), 680 (0.09), 528 (0.27), 487 (0.40), 460 (0.45), 385 (0.60), 359 nm (1.00); ¹H-NMR Bacteriochlorin moiety: δ = 9.01/8.99 (each 1H, s, 5-H), 8.48/8.44 (each 1H, s, 10-H), 8.45/8.40 (each 1H, s, 20-H), 5.14, 5.06, 4.96, 4.90 (each 1H, d, J = 20 Hz, 13¹-CH₂), 4.98 (2H, s, 17²-COOCH₂), 4.36-4.25 (4H, m, 7-, 18-H), 4.17/4.11 (each 1H, br-d, J = 9 Hz, 17-H), 4.05-4.03/4.02-3.98 (each 1H, m, 8-H), 3.51/3.48 (each 3H, s, 2-CH₃), 3.46/3.42 (each 3H, s, 12-CH₃), 3.17/3.15 (each 3H, s, 3¹-CH₃), 2.66-2.48, 2.31-2.18 (each 4H, m, 17-CH₂CH₂), 2.40-2.33, 2.12-2.06 (each 2H, m, 8-CH₂), 1.82/1.78 (each 3H, d, J = 7 Hz, 7-CH₃), 1.76/1.70 (each 3H, d, J = 7 Hz, 18-CH₃), 1.12/1.07 (each 3H, t, J = 7 Hz, 8¹-CH₃), 0.31, 0.30, -1.01, -1.08 (each 1H, s, NH \times 4), Carotenoid moiety: δ = 6.66 (1H, dd, J = 12, 15 Hz, 11[']-H), 6.63 (1H, dd, J = 12, 15 Hz, 15[']-H), 6.61 (1H, dd, J = 12, 13 Hz, 11^{''}-H), 6.50 (1H, dd, J = 12, 14 Hz, 15^{''}-H), 6.39 (1H, d, J = 15 Hz, 12^{''}-H), 6.34 (1H, d, J = 15 Hz, 12[']-H), 6.28 (1H, d, J = 12 Hz, 14[']-H), 6.23 (1H, d, J = 12 Hz, 14^{''}-H), 6.20 (each 1H, d, J = 15 Hz, 7^{''}-, 10^{''}-H), 6.16 (1H, d, J = 11 Hz, 10[']-H), 6.14 (1H, d, J = 16 Hz, 8^{''}-H), 6.08, 1H, d, J = 16 Hz, 7[']-H), 5.97 (1H, d, J = 16 Hz, 8[']-H), 4.96-4.90 (1H, m, 3[']-H), 2.30-2.26 (1H, m, 4[']-H _{α}), 2.03 (1H, t, J = 7 Hz, 4^{''}-H₂), 1.98 (3H, s, 19^{''}-H₃), 1.96 (3H, s, 20[']-H₃), 1.94-1.88 (1H, m, 4[']-H _{β}), 1.84 (3H, s, 20^{''}-H₃), 1.73 (3H, s, 18^{''}-H₃), 1.65-1.61 (2H, m, 3^{''}-H₂), 1.58 (3H, s, 18[']-H₃), 1.52, (1H, br-d, J = 14 Hz, 2[']-H _{α}), 1.49-1.46 (2H, m, 2^{''}-H₂), 1.33 (1H, t, J = 12 Hz, 2[']-H _{β}), 1.04 (each 3H, s, 16^{''}-, 17^{''}-H₃), 0.89 (3H, s, 17[']-H₃), 0.79 (3H, s,

16'-H₃); ¹³C-NMR quaternary carbon: $\delta = 199.2, 199.1, 195.7, 195.5, 173.0, 172.8, 170.4, 170.3, 168.6, 168.4, 163.57, 163.55, 157.3, 157.2, 147.2, 147.1, 139.1, 137.9, 137.6, 137.53, 137.46, 137.1, 136.5, 136.4, 136.3, 135.8, 135.73, 135.68, 132.73, 132.66, 132.1, 130.2, 129.4, 125.8, 120.9, 109.1, 109.0, 36.6, 34.3$ (three peaks are overlapping), Bacteriochlorin moiety: $\delta = 99.2/99.1$ (C10), 97.2 (C5), $95.92/95.89$ (C20), 58.6 (C17⁵), $55.03/55.00$ (C8), $51.22/51.19$ (C17), $49.5/49.4, 48.72/48.67$ (C7, 18), $47.8/47.6$ (C13²), $33.33/33.31$ (C3²), $31.3/31.0, 30.2/30.1, 30.0/29.9$ (C8¹, 17¹, 17²), $23.00, 22.98$ (C7¹, 18¹), 13.4 (C2¹), $11.5/11.4$ (C12¹), $10.8/10.7$ (C8²), Carotenoid moiety: $\delta = 140.6$ (C12^{''}), 137.7 (C8^{''}), 137.1 (C12[']), 135.5 (C8[']), 135.2 (C14[']), 134.2 (C14^{''}), 132.2 (C10^{''}), 131.0 (C11^{''}), 130.8 (C10[']), 129.6 (C15^{''}), 126.8 (C7^{''}), 126.2 (C7[']), 125.4 (C11[']), 123.2 (C15[']), 68.5 (C3[']), 43.7 (C2[']), 39.6 (C2^{''}), 38.3 (C4[']), 33.1 (C4^{''}), 19.2 (C3^{''}), 29.7 (C16[']), 28.3 (C17[']), 29.0 (C16^{''}, 17^{''}), 21.8 (C18^{''}), 21.3 (C18[']), $12.80, 12.76, 12.74$ (C19^{''}, 20^{''}, 20[']); HRMS m/z 1636.9537 (M⁺), calcd for C₁₀₆H₁₂₄N₈O₈⁺: 1636.9537.

REFERENCES

(S1) Tamiaki, H.; Kouraba, M.; Takeda, K.; Kondo, S.; Tanikaga, R., Asymmetric synthesis of methyl bacteriopheophorbide-*d* and analogues by stereoselective reduction of the 3-acetyl to the 3-(1-hydroxyethyl) group, *Tetrahedron: Asymmetry* **1998**, *9*, 2101-2111.

(S2) Karagiannidou, E.; Størseth, T. R.; Sliwka, H.-R.; Partali, V.; Malterud, K. E.; Tsimidou, M., Synthesis of two modified carotenoids and their behaviour during light exposure, *Eur. J. Lipid Sci. Technol.* **2003**, *105*, 419-426.

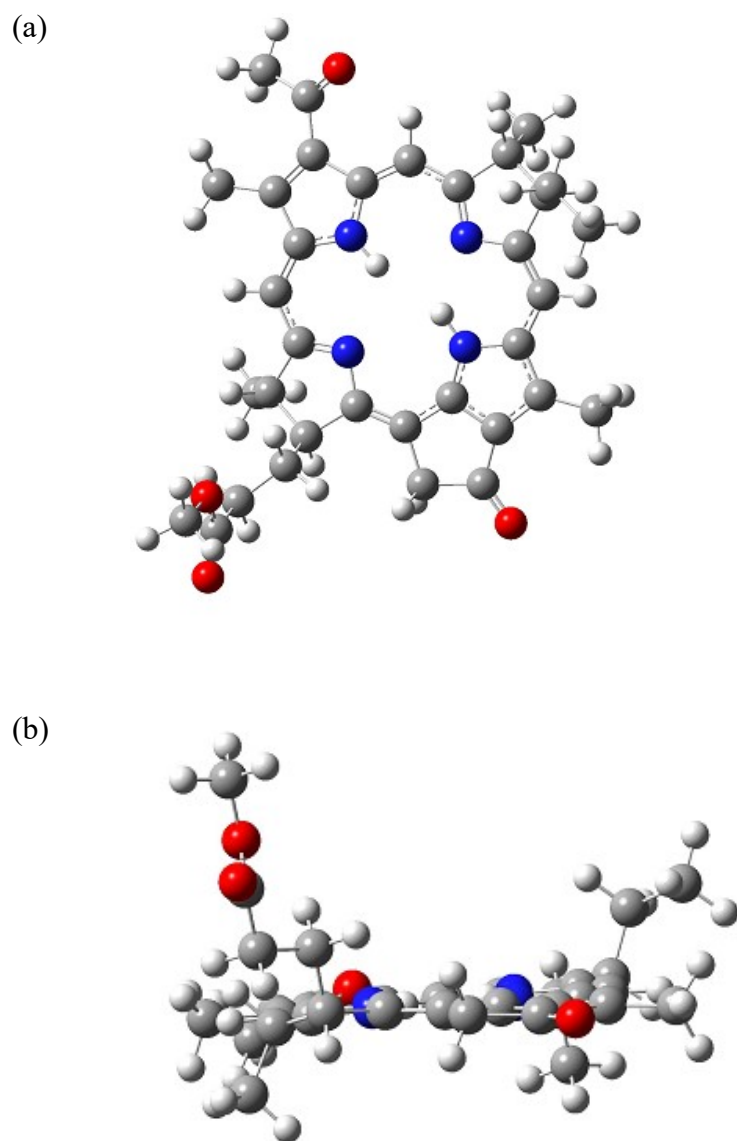


Figure S1. (a) Top view and (b) side view of the energy-optimized structure of **Dye-1** based on DFT calculation (the CAM-B3LYP exchange-correlations function and the 6-31G (d, p) basis set in the PCM (water)).

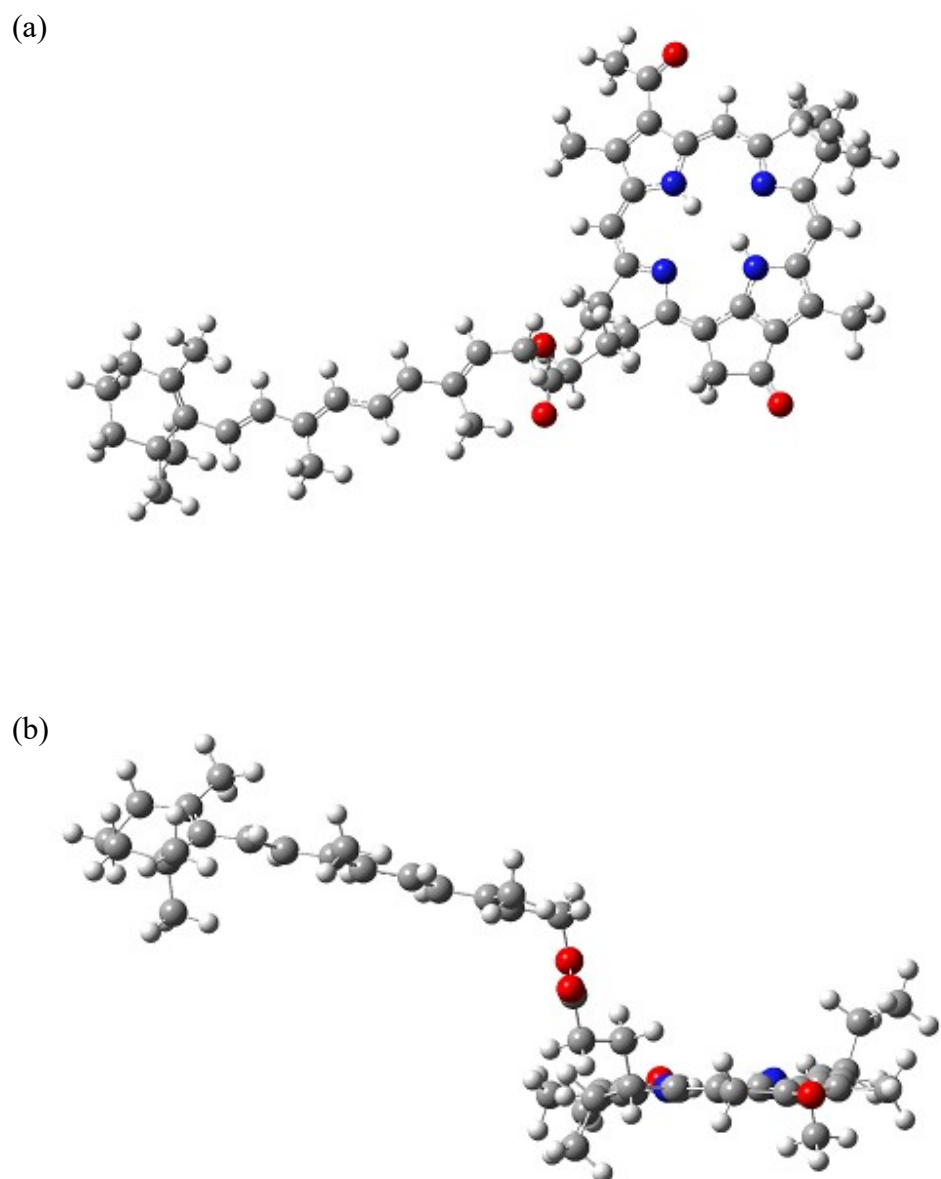
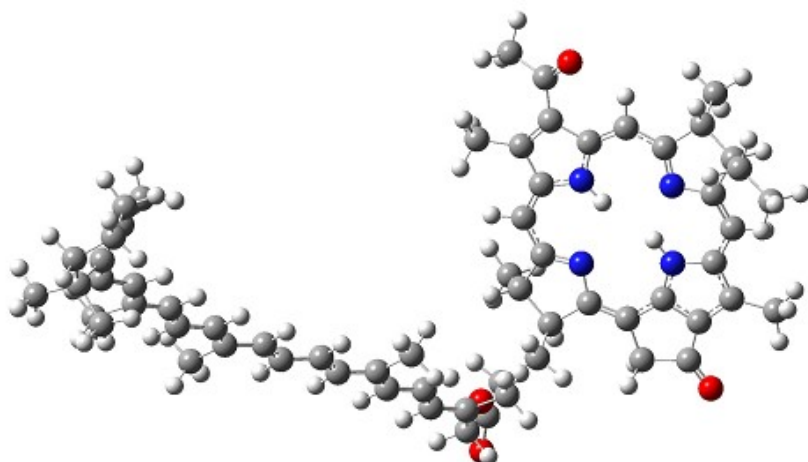


Figure S2. (a) Top view and (b) side view of the energy-optimized structure of **Dye-2** based on DFT calculation (the CAM-B3LYP exchange-correlations function and the 6-31G (d, p) basis set in the PCM (water)).

(a)



(b)

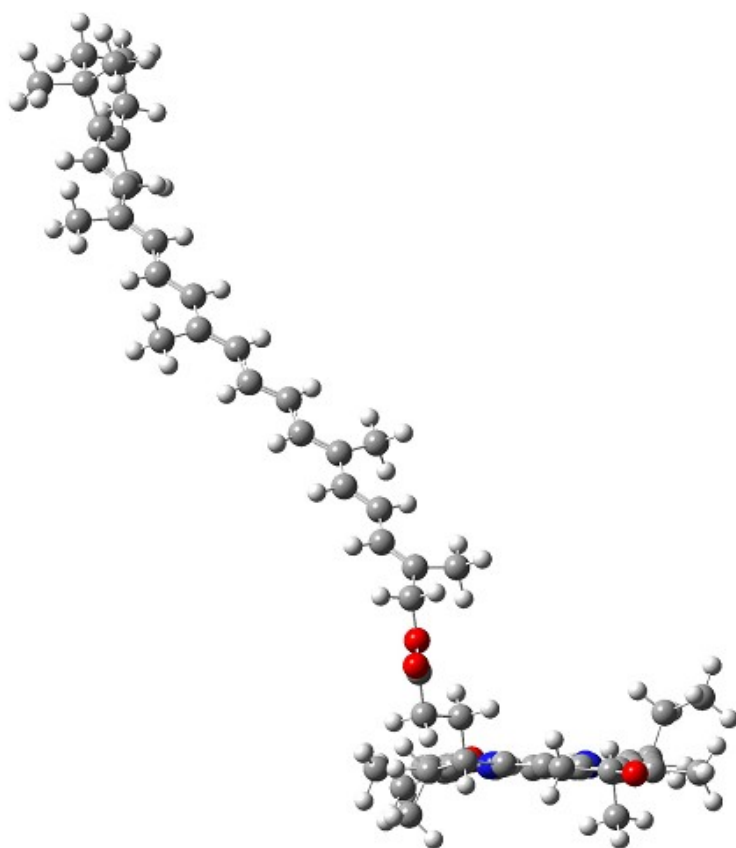


Figure S3. (a) Top view and (b) side view of the energy-optimized structure of **Dye-3** based on DFT calculation (the CAM-B3LYP exchange-correlations function and the 6-31G (d, p) basis set in the PCM (water)).

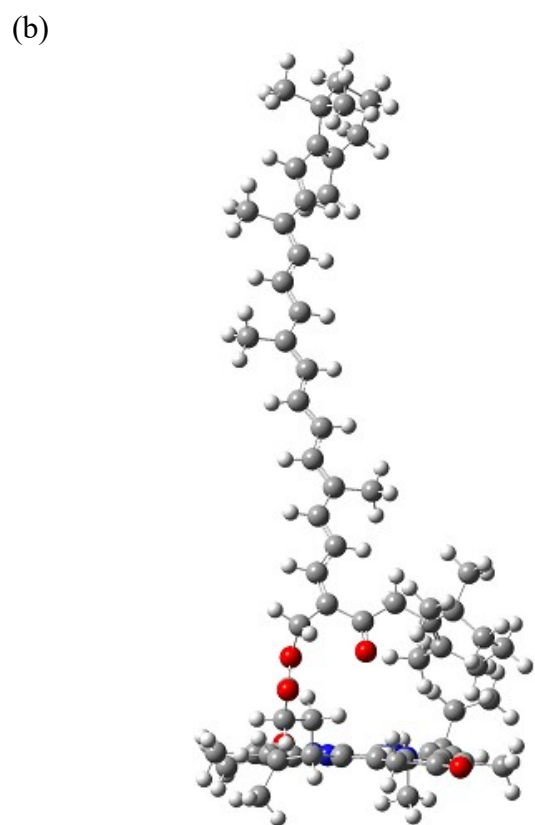
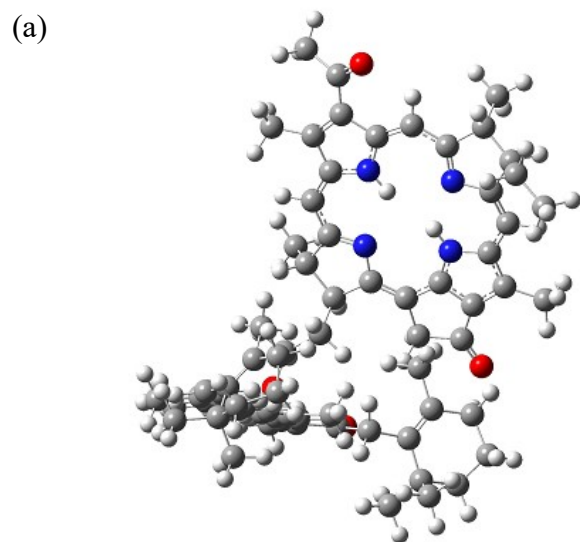


Figure S4. (a) Top view and (b) side view of the energy-optimized structure of **Dye-4** based on DFT calculation (the CAM-B3LYP exchange-correlations function and the 6-31G (d, p) basis set in the PCM (water)).

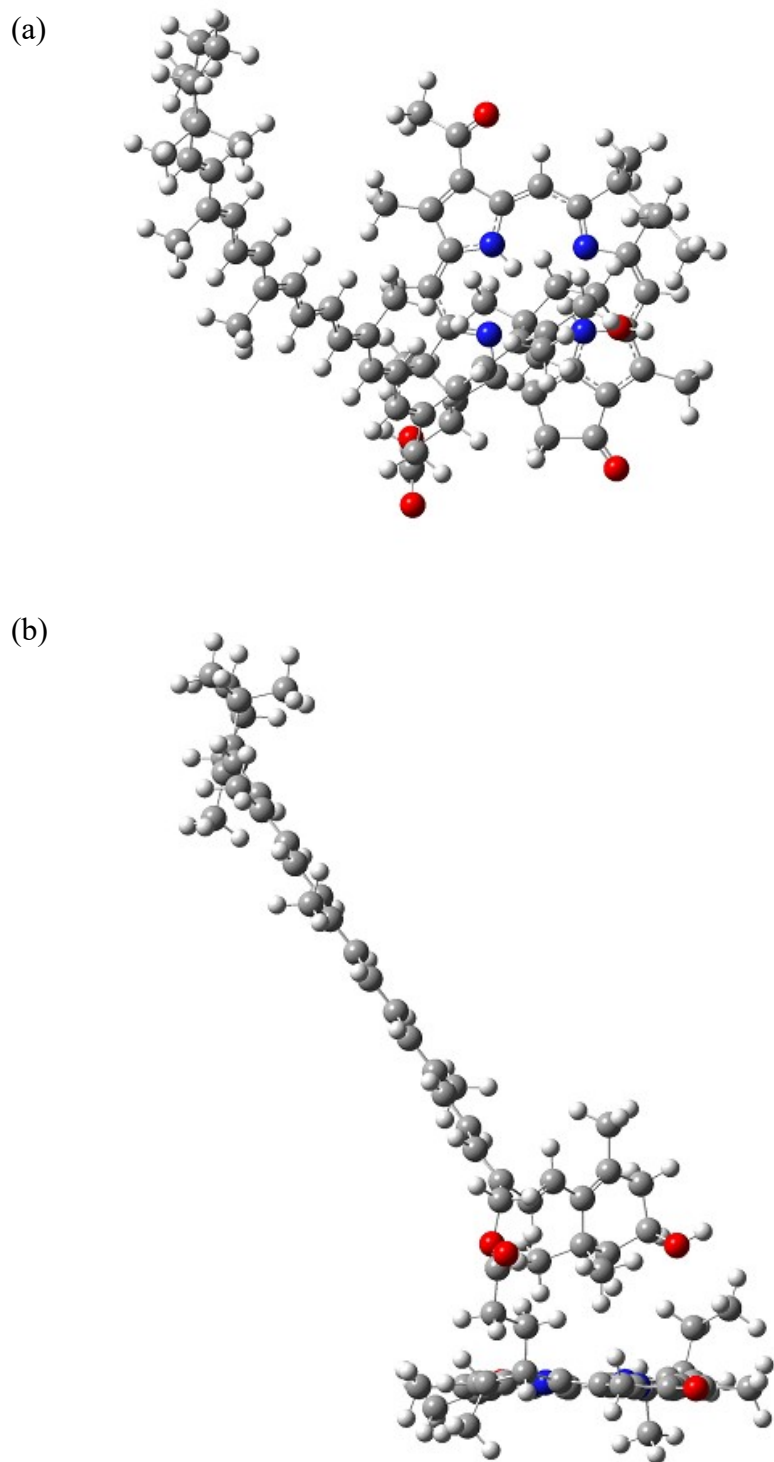


Figure S5. (a) Top view and (b) side view of the energy-optimized structure of **Dye-5** based on DFT calculation (the CAM-B3LYP exchange-correlations function and the 6-31G (d, p) basis set in the PCM (water)).

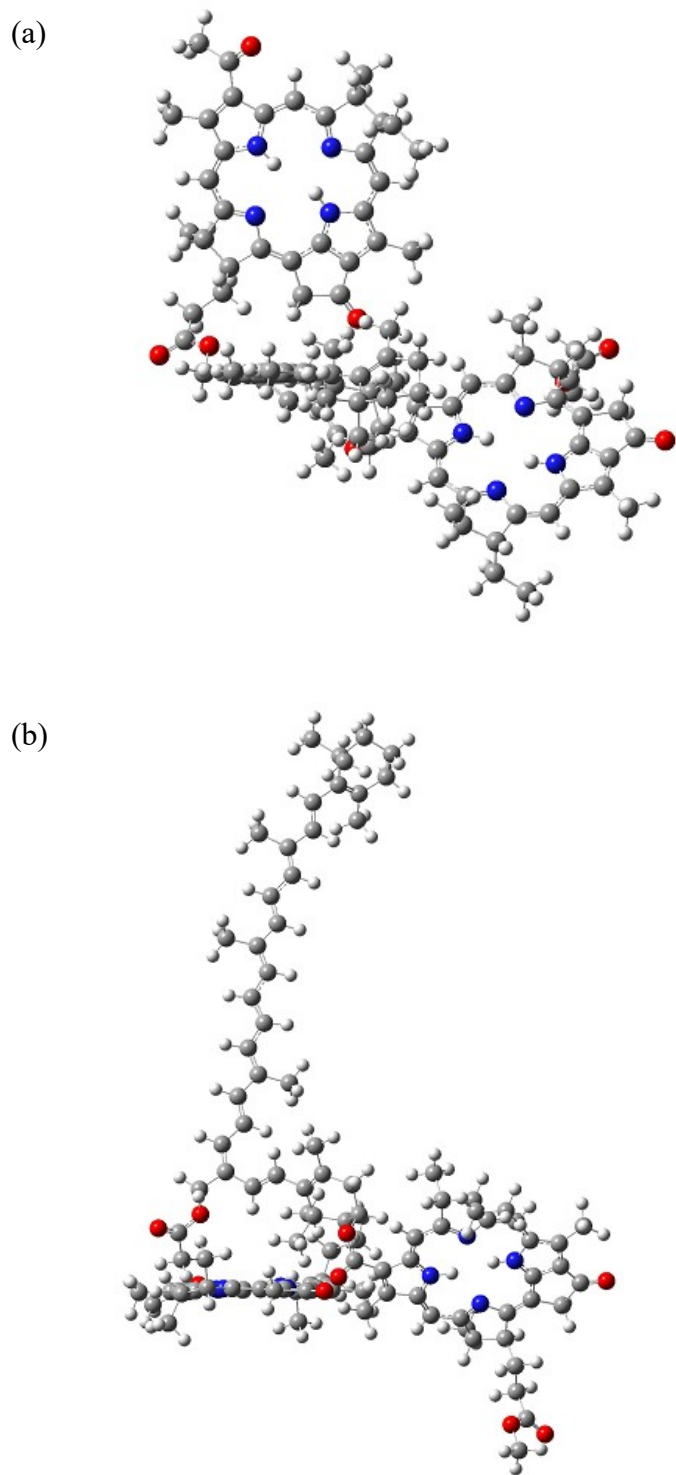


Figure S6. (a) Top view and (b) side view of the energy-optimized structure of **Dye-6** based on DFT calculation (the CAM-B3LYP exchange-correlations function and the 6-31G (d, p) basis set in the PCM (water)).

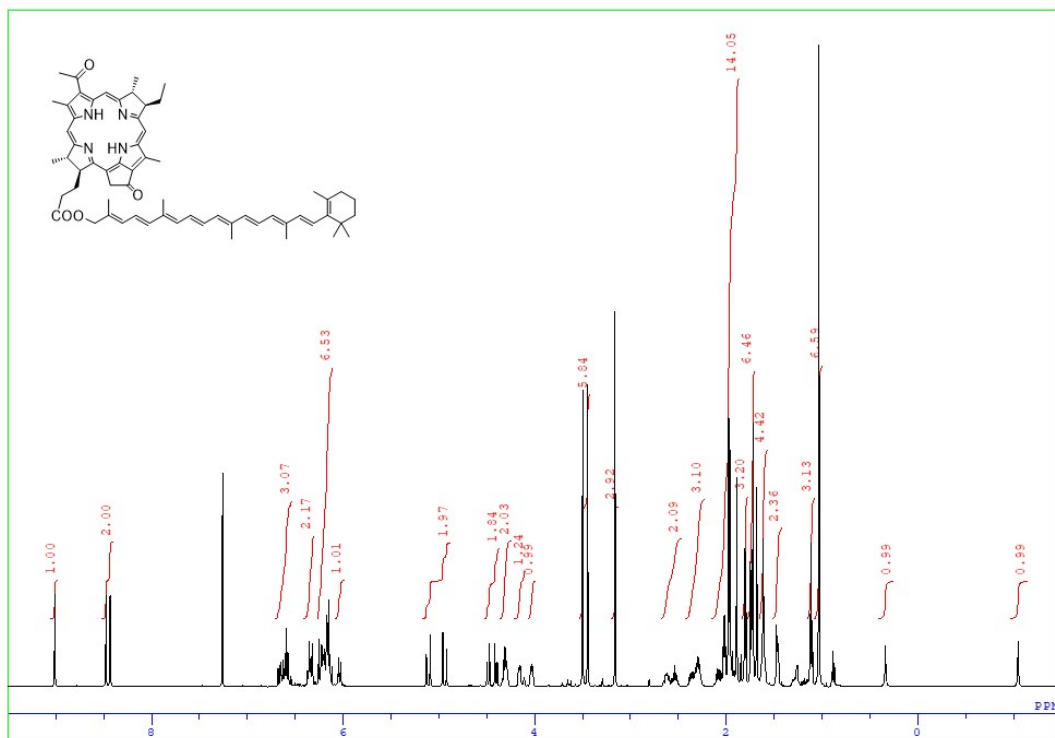


Figure S9. ¹H-NMR spectrum of **Dye-3** in CDCl₃.

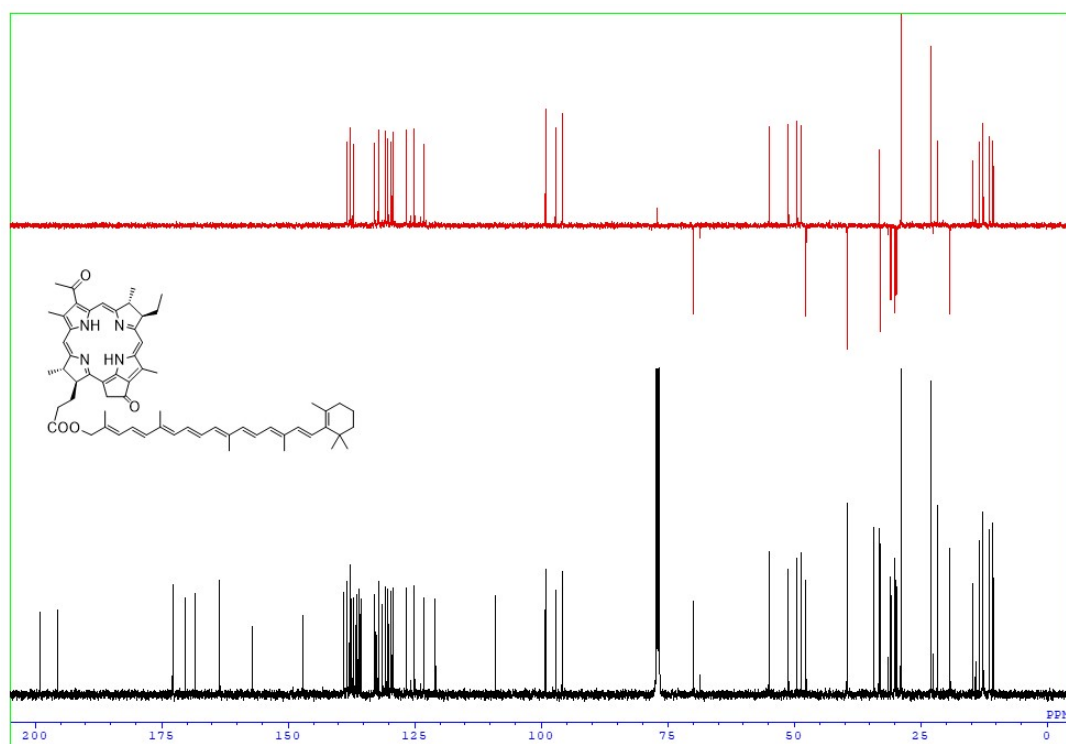


Figure S10. ¹³C-NMR spectrum of **Dye-3** in CDCl₃ (lower, black). Primary and tertiary carbon signals are shown upwards while secondary ones appear downwards in the DEPT spectrum (upper, red).

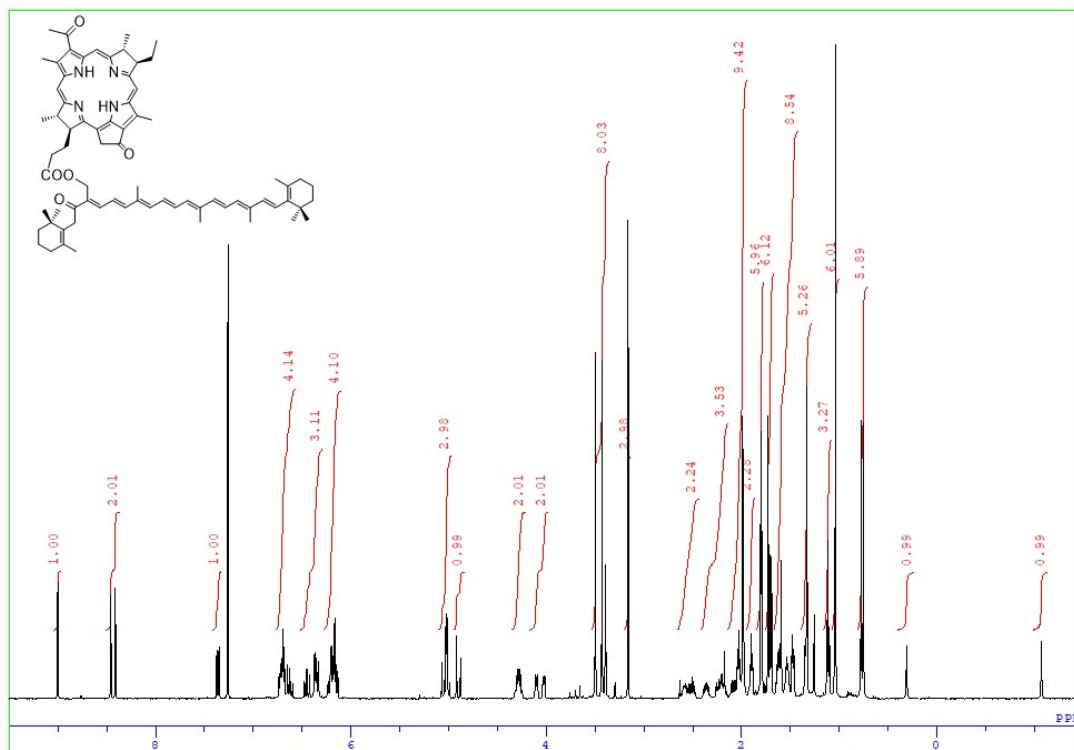


Figure S11. ¹H-NMR spectrum of **Dye-4** in CDCl₃.

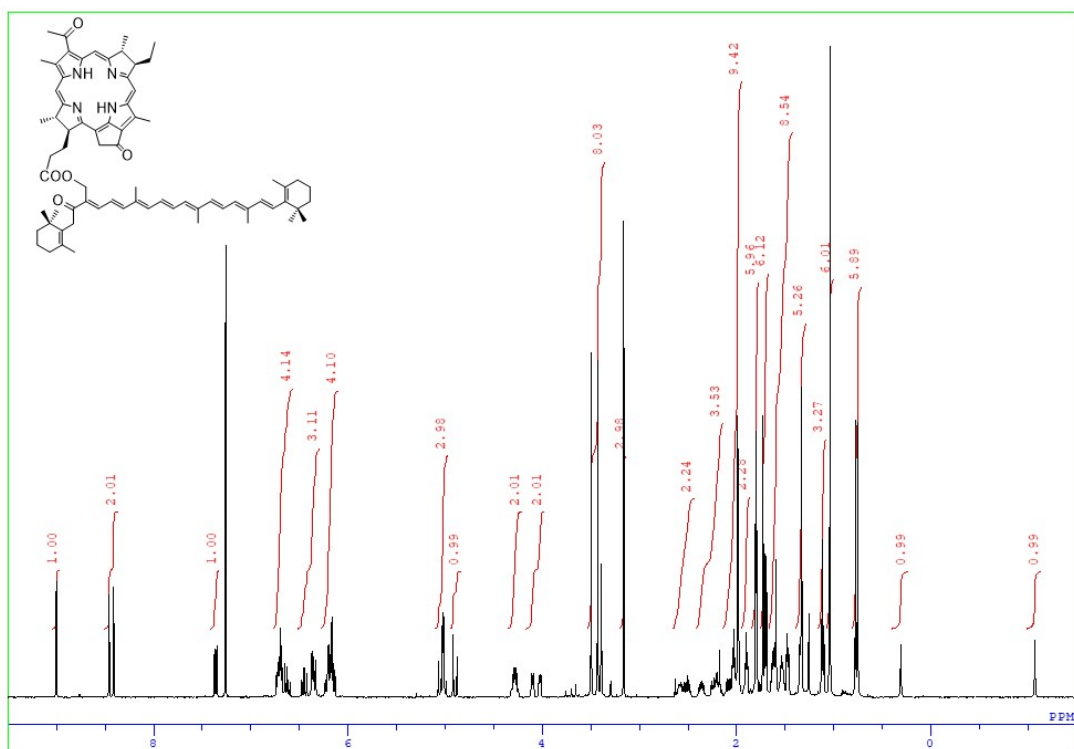


Figure S12. ¹³C-NMR spectrum of **Dye-4** in CDCl₃ (lower, black). Primary and tertiary carbon signals are shown upwards while secondary ones appear downwards in the DEPT spectrum (upper, red).

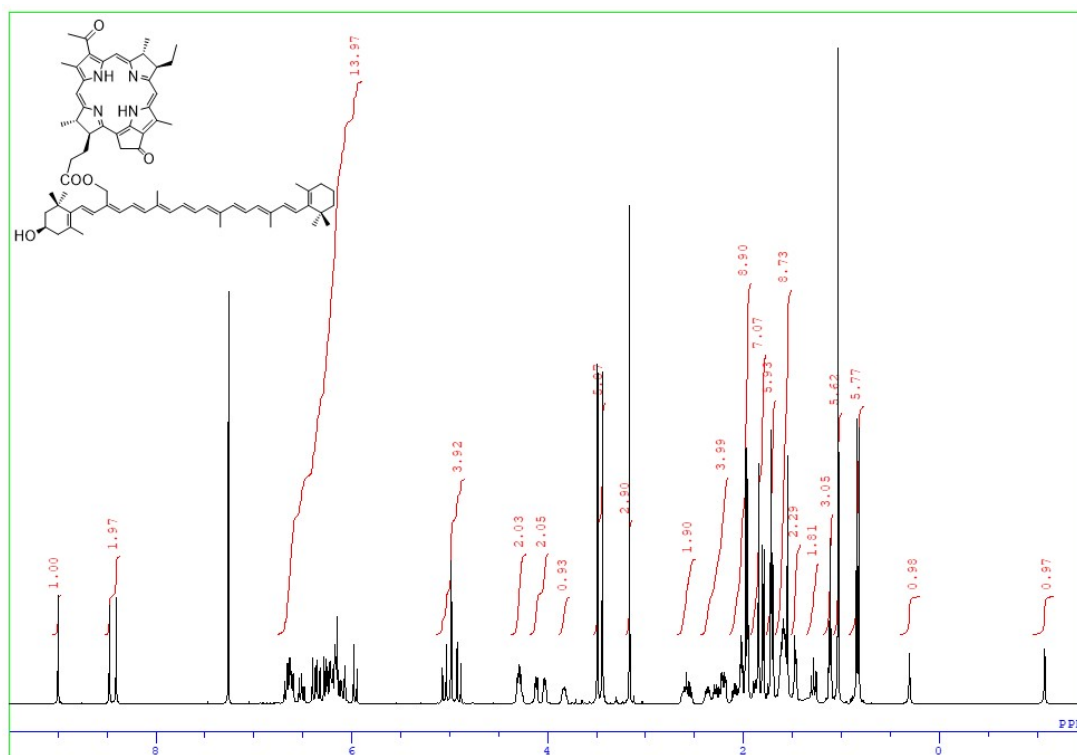


Figure S13. ^1H -NMR spectrum of **Dye-5** in CDCl_3 .

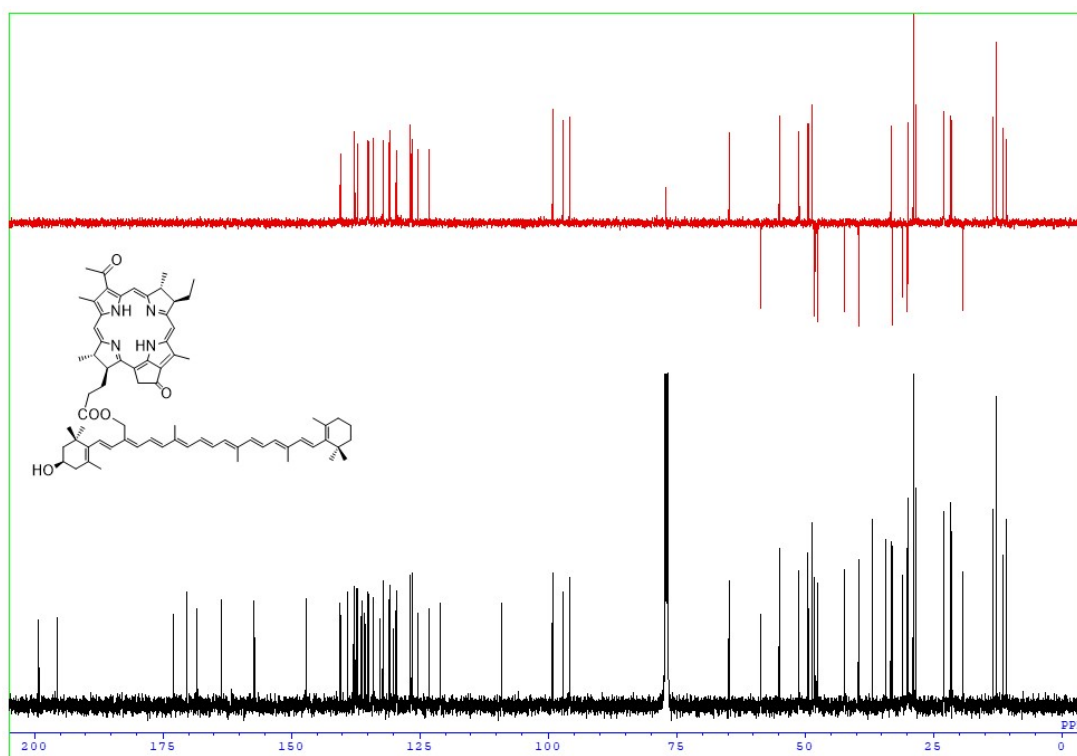


Figure S14. ^{13}C -NMR spectrum of **Dye-5** in CDCl_3 (lower, black). Primary and tertiary carbon signals are shown upwards while secondary ones appear downwards in the DEPT spectrum (upper, red).

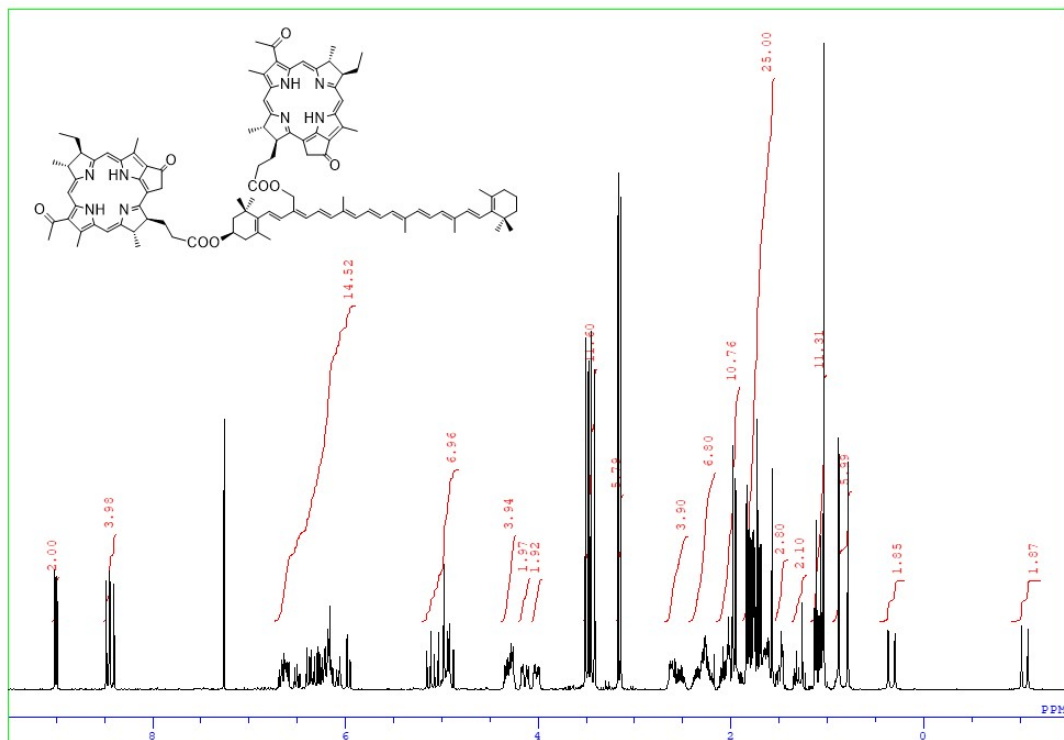


Figure S15. $^1\text{H-NMR}$ spectrum of **Dye-6** in CDCl_3 .

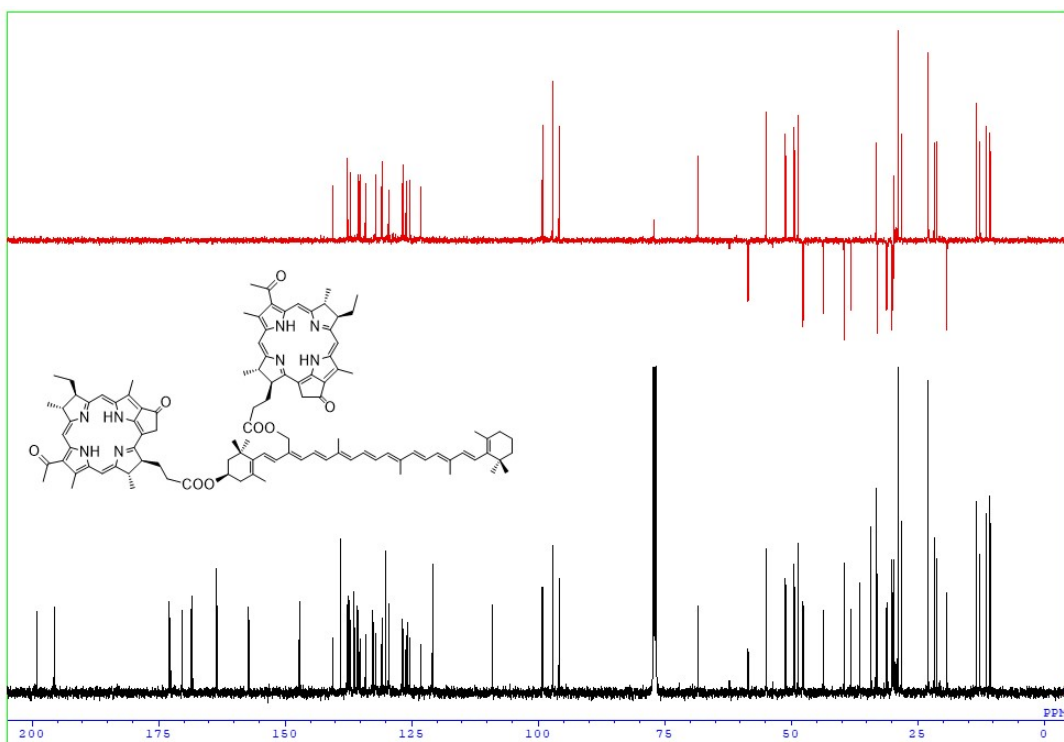


Figure S16. $^{13}\text{C-NMR}$ spectrum of **Dye-6** in CDCl_3 (lower, black). Primary and tertiary carbon signals are shown upwards while secondary ones appear downwards in the DEPT spectrum (upper, red).

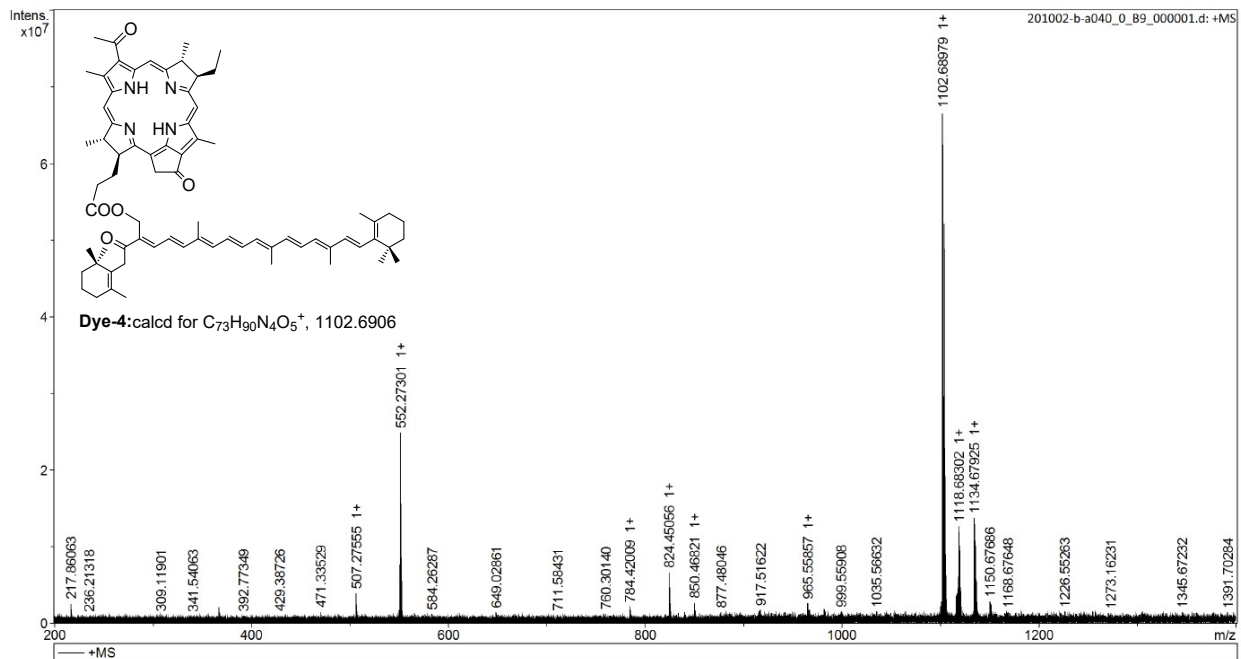


Figure S19. HRMS spectrum of **Dye-4**.

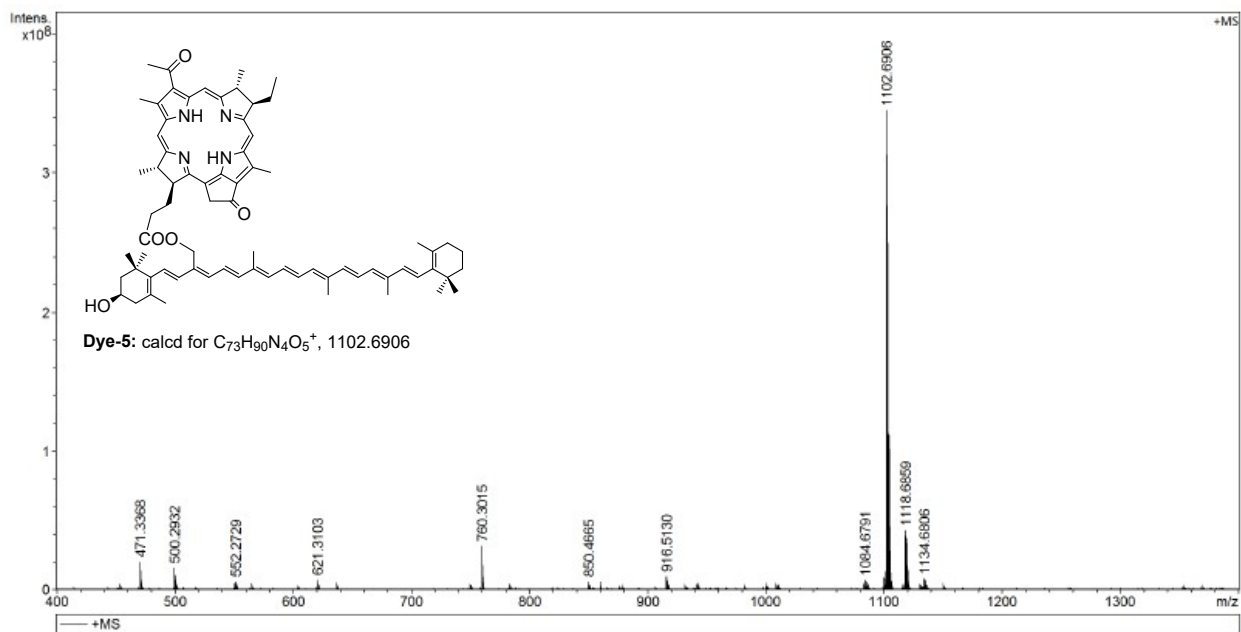


Figure S20. HRMS spectrum of **Dye-5**.

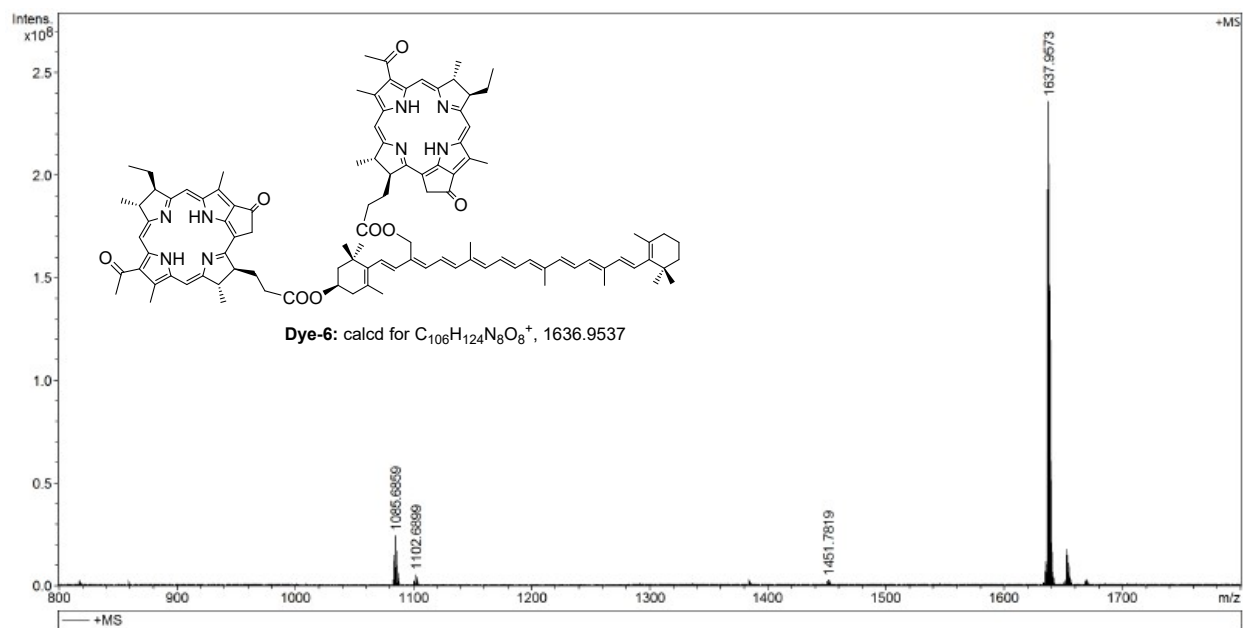


Figure S21. HRMS spectrum of **Dye-6**.

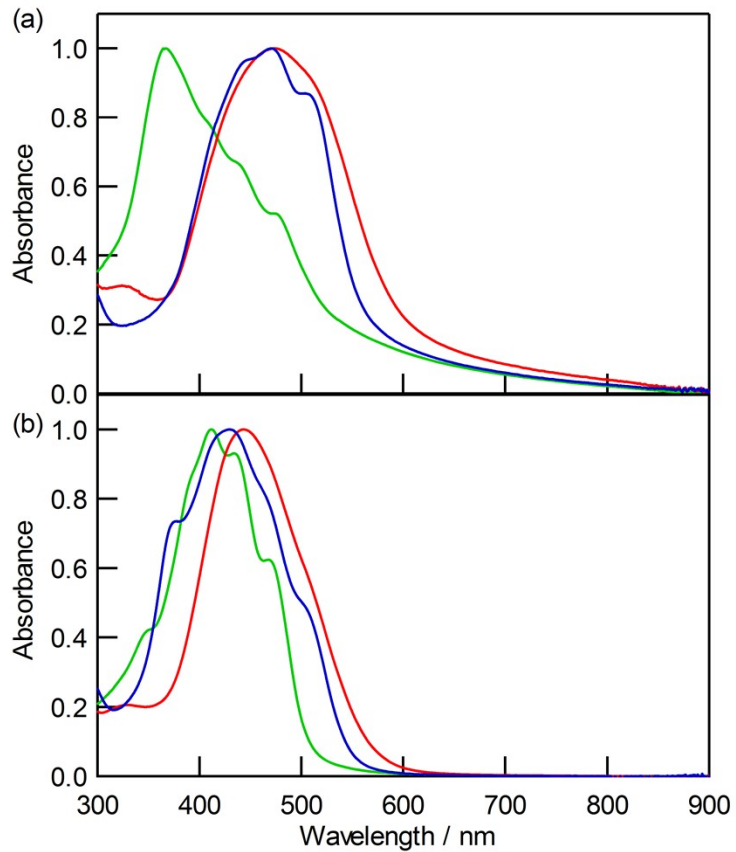


Figure S22. UV-VIS absorption spectra of β -apo-8'-carotenol **3** (green), siphonaxanthin analog **4** (red), and loroxanthin analog **5** (blue) (a) in the solid thin film and (b) in 1% THF-H₂O.

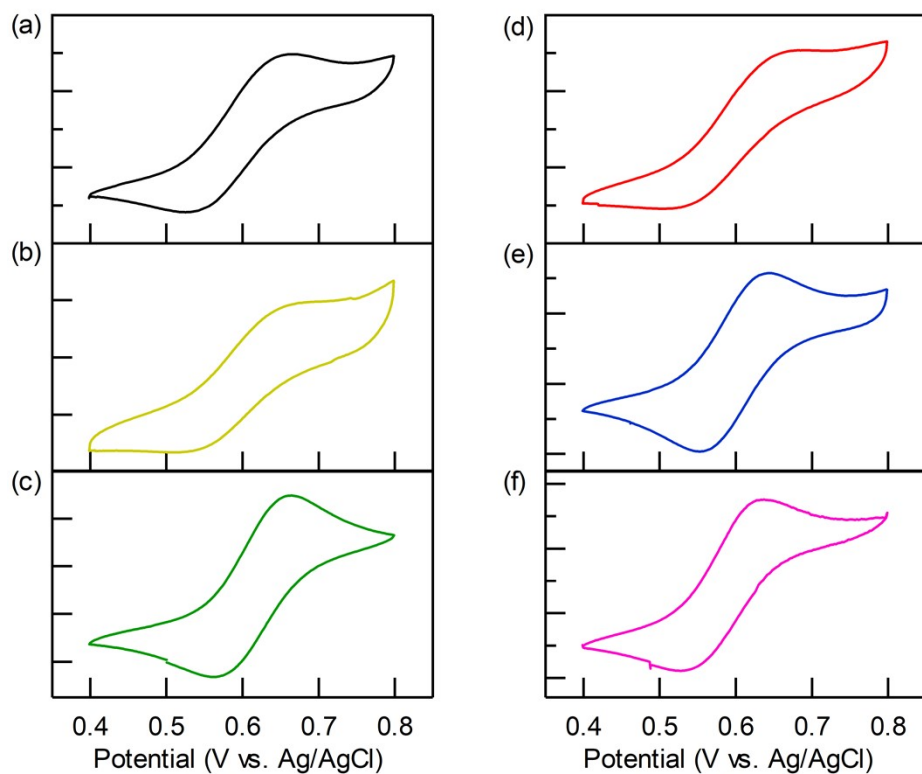


Figure S23 Cyclic voltammograms of (a) **Dye-1**, (b) **Dye-2**, (c) **Dye-3**, (d) **Dye-4**, (e) **Dye-5**, and (f) **Dye-6** in CH_2Cl_2 with 0.1 M tetrabutylammonium hexafluorophosphate as a supporting electrolyte at a scan rate of 100 mV/s.

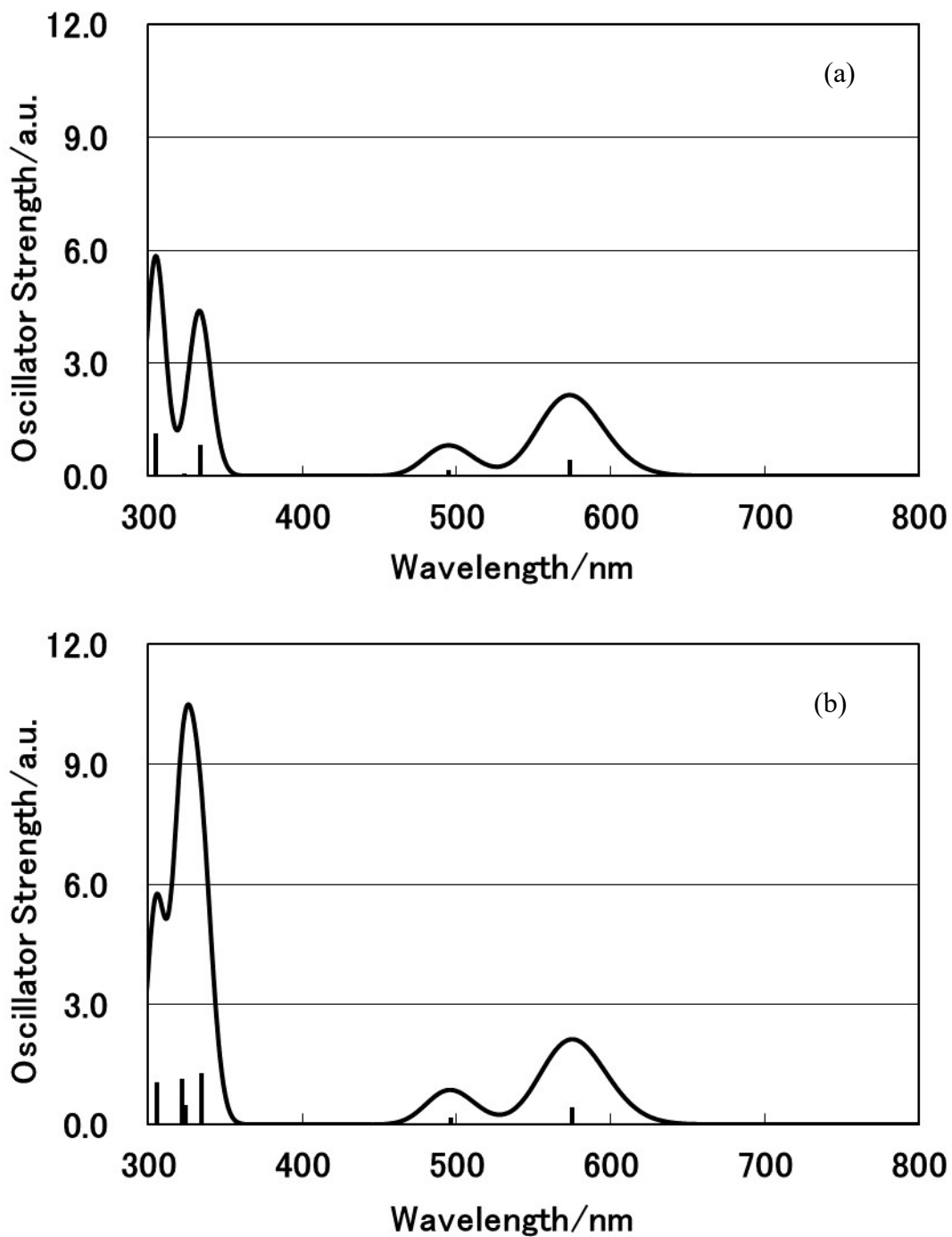


Figure S24. Theoretical absorption spectra and oscillator strength based on TD-DFT/CAM-B3LYP/6-31G(d,p) in the PCM (water) for (a) **Dye-1** and (b) **Dye-2**.

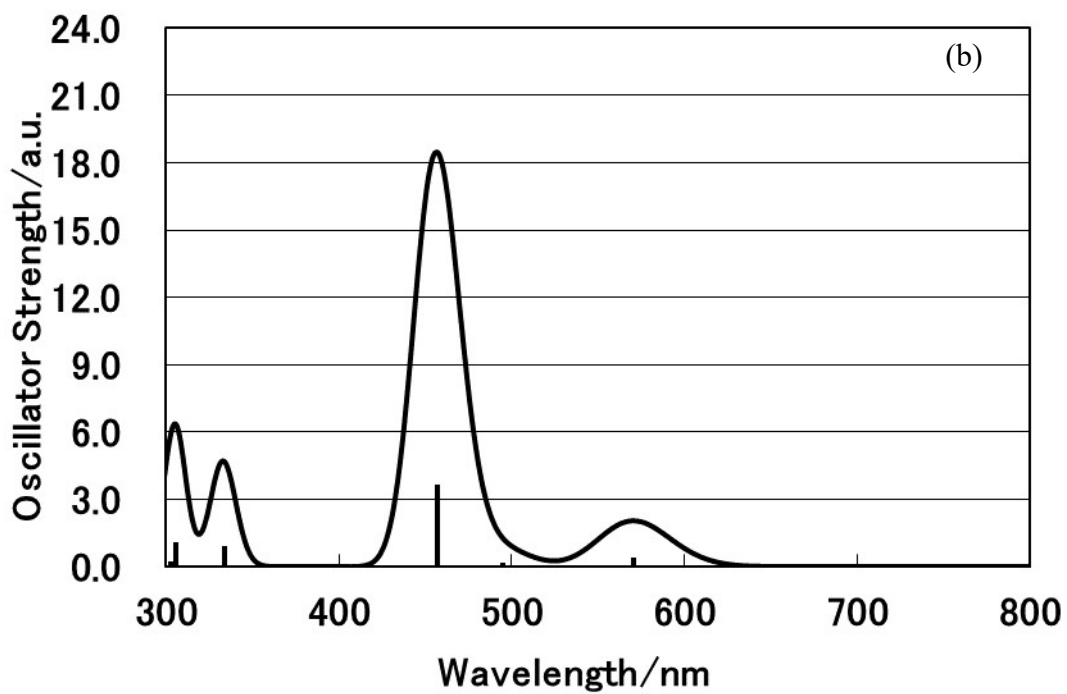
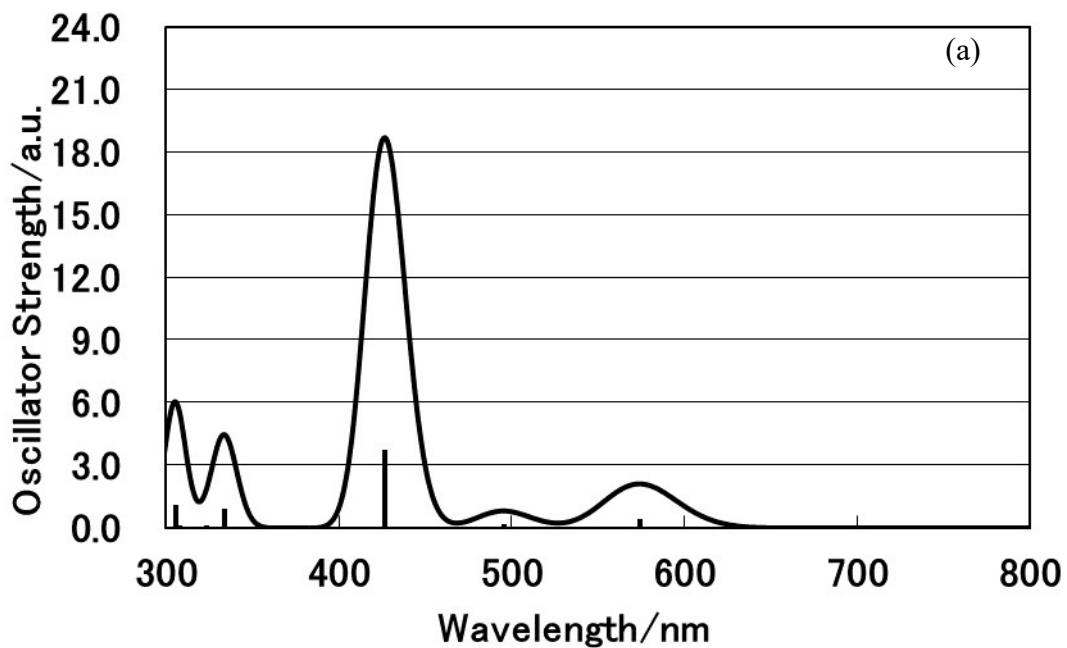


Figure S25. Theoretical absorption spectra and oscillator strength based on TD-DFT/CAM-B3LYP/6-31G(d,p) in the PCM (water) for (a) **Dye-3** and (b) **Dye-4**.

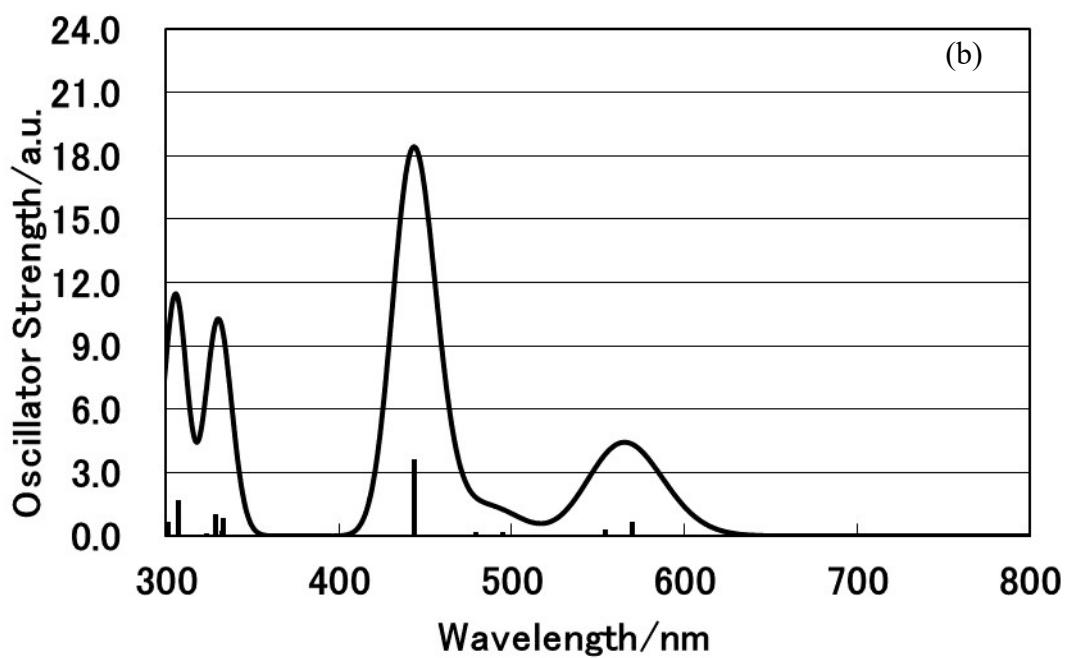
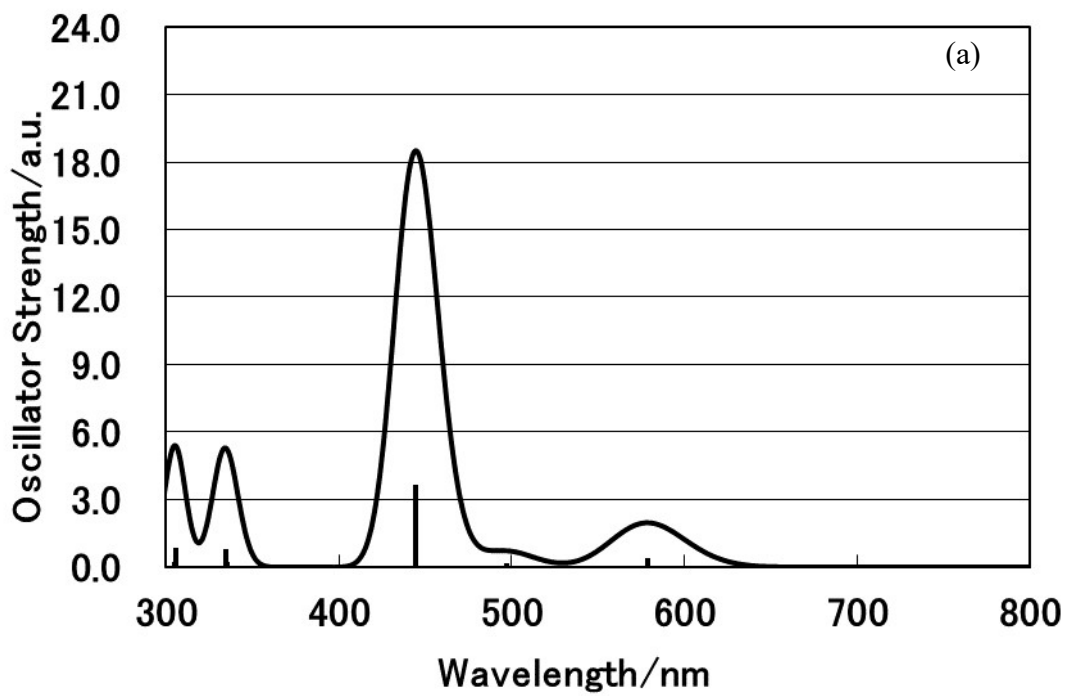


Figure S26. Theoretical absorption spectra and oscillator strength based on TD-DFT/CAM-B3LYP/6-31G(d,p) in the PCM (water) for (a) **Dye-5** and (b) **Dye-6**.

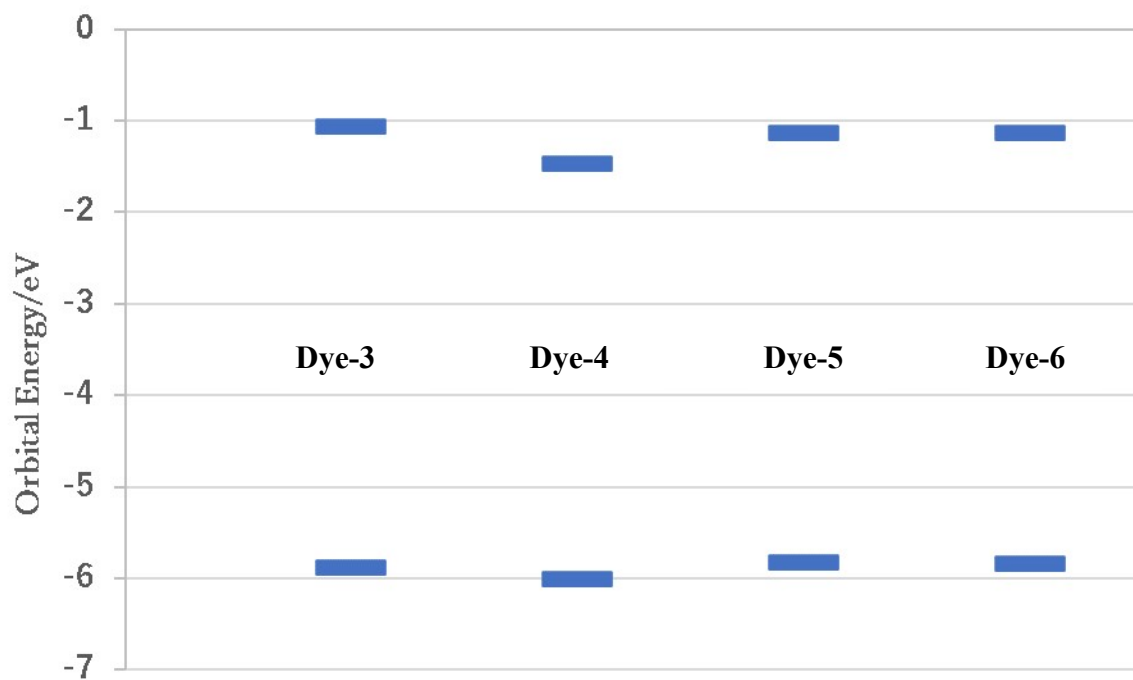


Figure S27. Energy gaps concerning main contributed frontier orbitals describing the electron excitations in the carotenoid moieties of **Dyes-3-6** based on TD-DFT/CAM-B3LYP/6-31G(d,p) in the PCM (water).

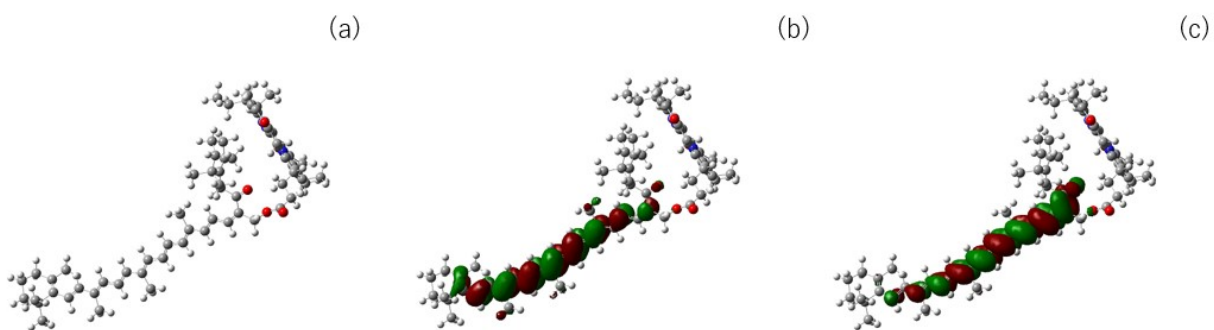


Figure S28. (a) Optimized structure, (b) (HOMO-1) orbital, and (c) (LUMO+1) orbital of **Dye-4** based on DFT/CAM-B3LYP/6-31G(d,p) in the PCM (water).

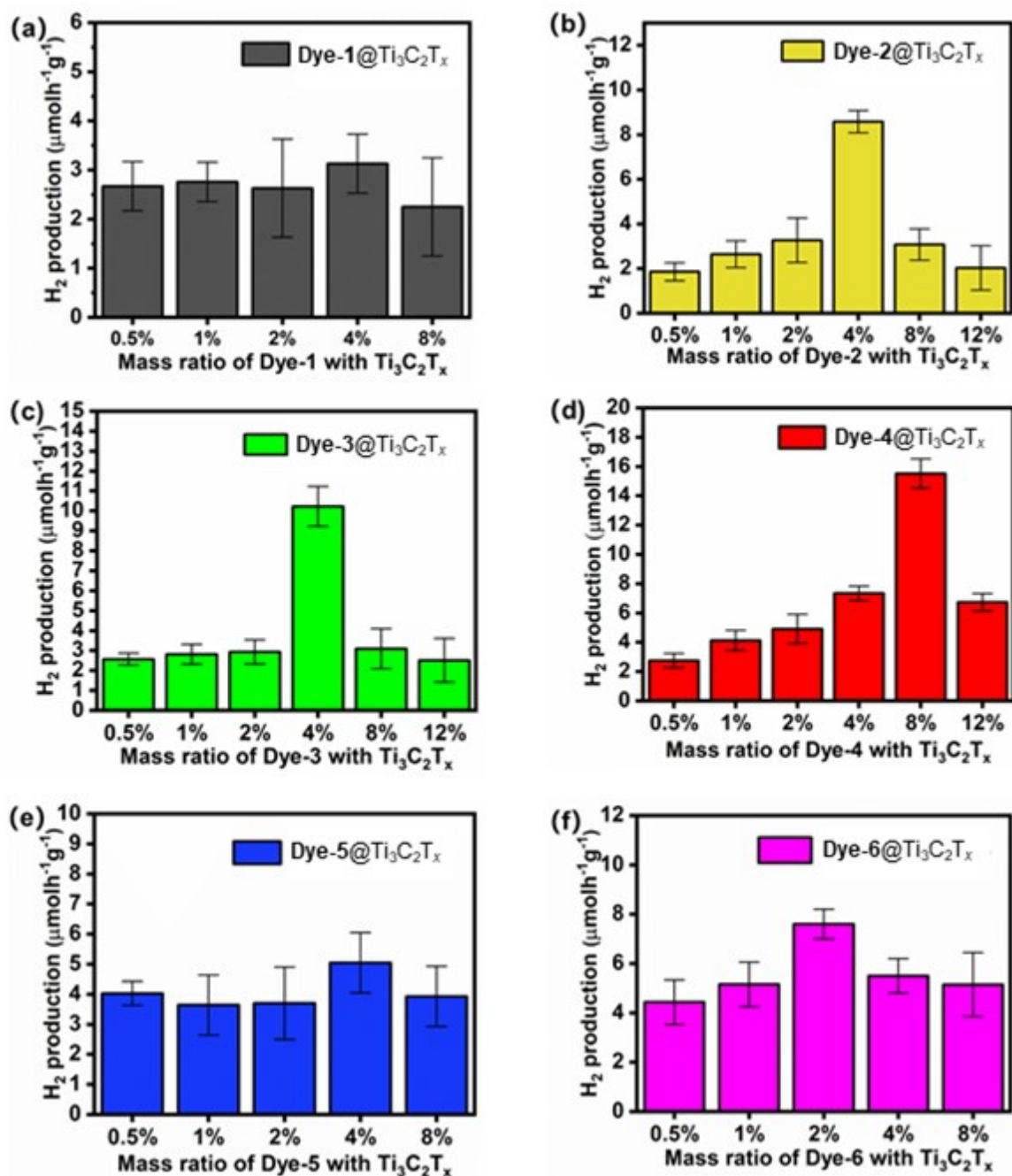


Figure S29. The hydrogen production of (a) **Dye-1@ $\text{Ti}_3\text{C}_2\text{T}_x$** , (b) **Dye-2@ $\text{Ti}_3\text{C}_2\text{T}_x$** , (c) **Dye-3@ $\text{Ti}_3\text{C}_2\text{T}_x$** , (d) **Dye-4@ $\text{Ti}_3\text{C}_2\text{T}_x$** , (e) **Dye-5@ $\text{Ti}_3\text{C}_2\text{T}_x$** , and (f) **Dye-6@ $\text{Ti}_3\text{C}_2\text{T}_x$** with different mass ratios under the white light illumination ($\lambda > 420 \text{ nm}$).

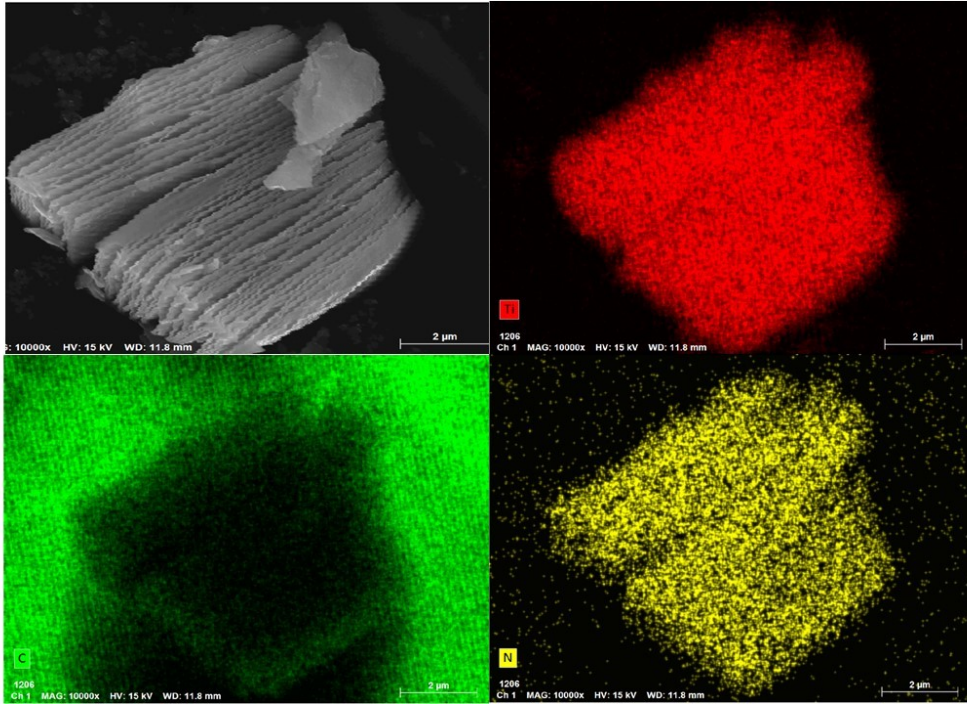


Figure S30. Elemental distribution mapping of Ti (upper right), C (lower left), and N (lower right) in **Dye-1**@ $\text{Ti}_3\text{C}_2\text{T}_x$, indicating that the N element is uniformly distributed on the surface of $\text{Ti}_3\text{C}_2\text{T}_x$ and therefore **Dye-1** is uniformly deposited on $\text{Ti}_3\text{C}_2\text{T}_x$.

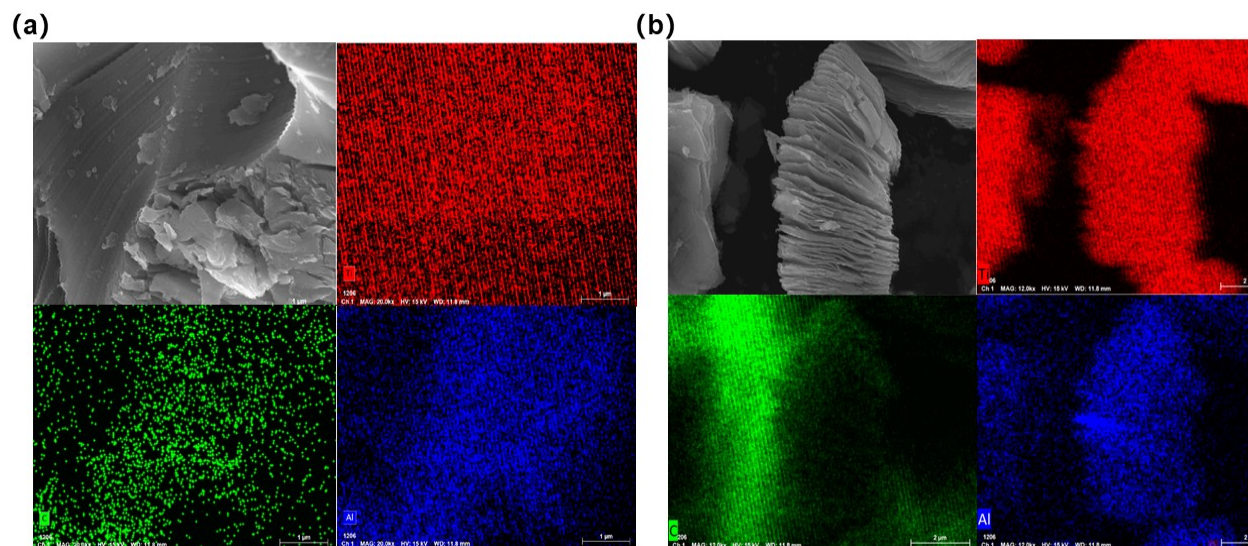


Figure S31. Elemental distribution mapping of Ti (upper right), C (lower left), and Al (lower right) in Ti_3AlC_2 and $\text{Ti}_3\text{C}_2\text{T}_x$, of which Al contents were analyzed to be 18.58% and 0.88%, respectively. The significantly reduced Al content after etching of Ti_3AlC_2 reveals the almost complete removal of the Al layer to turn into $\text{Ti}_3\text{C}_2\text{T}_x$.

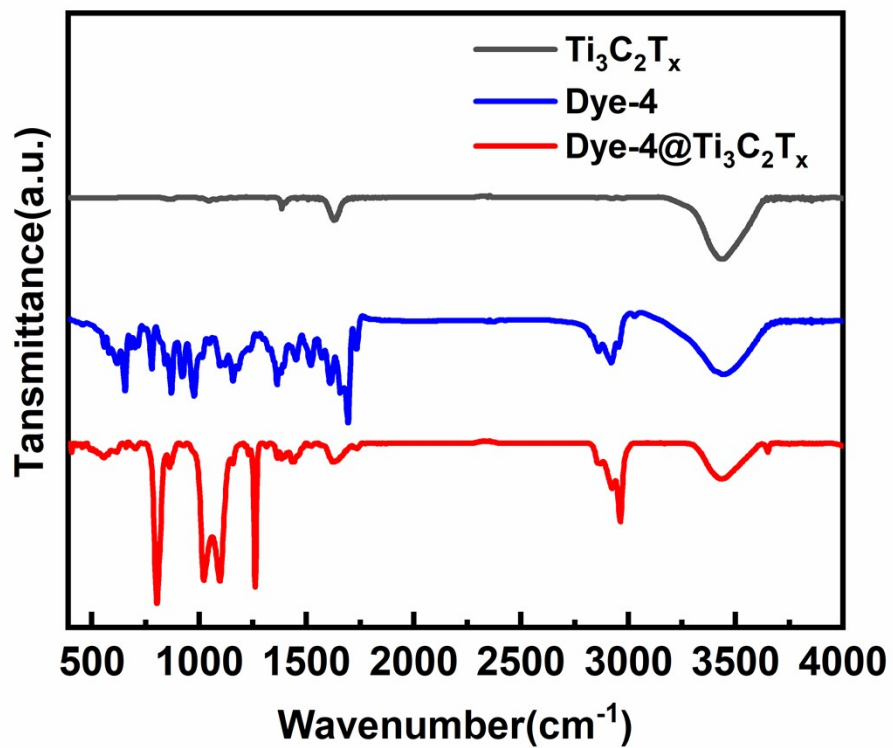


Figure S32. FT-IR spectra of Ti₃C₂T_x, Dye-4, and Dye-4@Ti₃C₂T_x.

Table S1. The fitting data of Nyquist plots for **Dye-1@Ti₃C₂T_x**, **Dye-3@Ti₃C₂T_x**, **Dye-4@Ti₃C₂T_x**, and **Dye-5@Ti₃C₂T_x**.

Composit	R ₁ /Ω	R ₂ /Ω	CPE-T	CPE-P	W _O -R	W _O -T	W _O -P
Dye-1@Ti₃C₂T_x	44.9	51.8	0.000181	0.758	315	38.5	0.408
Dye-3@Ti₃C₂T_x	17.6	10.1	0.001432	0.519	16.9	0.363	0.382
Dye-4@Ti₃C₂T_x	23.0	6.1	0.000247	0.726	14.1	0.128	0.378
Dye-5@Ti₃C₂T_x	31.0	23.5	0.000391	0.495	0.174	0.000519	0.350